Faculty of Medicine and Dentistry

Department of Internal Medicine and Medical Specialties

PhD in Arterial Hypertension and Vascular Biology (ARHYAVB)

XXXVII course

"SECONDARY BRAIN INJURY AFTER PARENCHYMAL CEREBRAL HEMORRHAGE IN HUMANS: THE ROLE OF NOX2-MEDIATED OXIDATIVE STRESS AND ENDOTHELIN-1"

Supervisor:

Prof. Danilo Toni

Co-supervisor:

Dr. M. De Michele

PhD student:

Dr. Irene Berto

1307940

Academic Year 2024/2025

SUMMARY:

Abbreviations: Intraparenchymal cerebral hemorrhage (ICH); Endothelin-1 (ET-1); Nitrites/nitrates (NO), NADPH oxidase-2 (NOX-2); Asymmetric dimethylarginine (ADMA); Perihematomal edema (PHE); Blood-brain barrier (BBB); Red blood cells (RBCs); Positron Emission Tomography (PET); Diffusion-Weighted (DW) magnetic resonance imaging (MRI); Cerebral blood flow (CBF); Endothelin-1, endothelin-2 and endothelin-3 (ET-1, ET-2 and ET-3); Neuronal NOS (nNOS); Inducible NOS (iNOS); Central nervous system (CNS); peripheral nervous system (PNS); reactive oxygen species (ROS); Asymmetric dimethyl-arginine (ADMA); Nicotinamide adenine dinucleotide phosphate (NADPH), NADPH oxidase (NOX); secondary brain injury (SBI); reactive oxygen species (ROS); National Institutes of Health Stroke Scale (NIHSS); brain Computed Tomography (CT); Apparent diffusion coefficient (ADC); Fluid attenuated inversion recovery (FLAIR); Gradient Echo (GE); modified Rankin scale (mRS); Mean Transit Time (MTT); Cerebral Blood Flow (CBF); Cerebral Blood Volume (CBV).

1. ABSTRACT

Spontaneous intraparenchymal cerebral hemorrhage (ICH) accounts for about 20% of all stroke cases and is associated with high rates of mortality and long-term disability.

Despite a growing interest from the scientific community, currently no decisive therapeutic target has been established.

Perihematomal hypoperfusion may lead to ischemic damage during intraparenchymal cerebral hemorrhage (ICH), resulting in worse prognosis. We aimed to (1) investigate the relationship between serum biomarkers related to oxidative stress and vasoactive substances and the occurrence of hypoperfusion and ischemic perihematomal lesions in ICH, (2) to evaluate their correlation with the volumetric evolution of the hematoma and perihematomal edema.

We enrolled 28 patients affected by ICH. Blood samples were collected at three different timepoints from symptoms onset: T0, T1 and T2 (admission, 12-24hs and 48-72hs respectively), to measure Endothelin-1 (ET-1), nitrites/nitrates (NO), NADPH oxidase-2 (NOX-2), and asymmetric dimethylarginine (ADMA). Patients underwent brain MRI with perfusion study at T1 and MRI without perfusion at T2. 12 patients had ischemic perihematomal lesions at T1. A higher NOX-2 concentration at T0 was observed in patients with ischemic perihematomal lesions compared to those without, ($p=0.051$) and with a more severe perihematomal edema at T2 ($p=0.011$). The ischemic perihematomal lesions development was also associated with increased hematoma volume ($p<0.005$), perilesional edema ($p=0.046$), greater midline shift ($p=0.036$). ET-1 values at T1 inversely correlated with hemorrhage volume at T2 ($\rho=-0.717$, $p=0.030$).

NOX-2 may have a key role in the development of ischemic perihematomal lesions, aligning with previous research indicating that oxidative stress contributes to secondary brain injury in ICH.

The association between higher ET-1 values and a lower hemorrhage volume could be related to the ET-1 vasoconstriction action on the ruptured vessel wall.

2. INTRODUCTION

Spontaneous intraparenchymal cerebral hemorrhage (ICH) accounts for about 20% of all stroke cases and is associated with high rates of mortality and long-term disability (Feigin et al., 2021; Flaherty et al., 2006; Jolink et al., 2015; Zahuranec et al., 2014). Up to 50% of ICH patients die within 1 month after onset and residual disability is common among survivors (Van Asch et al., 2010)

Despite a growing interest from the scientific community on the topic of ICH, currently no decisive therapeutic target has been established.

The role of primary damage due to direct mechanical compression by the hematoma itself on the surrounding tissue is well established. In recent years, however, many studies have highlighted the importance of secondary damage whose physiopathology is not completely understood. Perihematomal edema (PHE) and hypoperfusion, oxidative stress, neuroinflammation, alteration of the blood-brain barrier (BBB), and vasoactive metabolites have been advocated (Bautista et al., 2021; Fainardi et al., 2008; Wilkinson et al., 2018).

Hypoperfusion, together with additional factors, i.e., cerebral microangiopathy and atherosclerosis, hyperglycemia, neuroinflammation, and oxidative stress, may also be the trigger for the development of silent ischemic lesions, localized both near and in remote regions from the hematoma (Boulanger et al., 2019; Yang et al., 2022). Although pathophysiology of perihematomal ischemic lesions development is not completely ascertained, the appearance of these lesions is associated with a worse prognosis and with the recurrence of cerebrovascular events (both ischemic and hemorrhagic), cognitive decline, and death (Boulanger et al., 2019; Menon et al., 2012; Prabhakaran and Naidech, 2012).

2.1 Pathophisiology of intraparenchimal hemorrage

Primary injury induced by ICH is due to the mass effect produced by extravasated blood during the acute phase (from minutes to hours after the bleeding onset). The sudden and rapid accumulation of

blood involves physical disruption of BBB, mechanical compression of adjacent tissue, and results in an increase of intracranial pressure. In the late acute and subacute phases secondary brain injury results in a variety of pathological pathways including iron-mediated oxidative stress, inflammatory response, excitotoxicity, cytotoxicity, spreading depression, and hypermetabolism (Lattanzi et al., 2020), which are responsible for development of the BBB dysfunction, PHE, and brain cell death, resulting in a worse prognosis. Inflammation plays a complex and ambivalent role in the progression of ICH. Inflammation can be detrimental (e.g., early brain injury and edema) and protective (e.g., clot and injury resolution) at the same time, after ICH. Accordingly, a better understanding of the pathophysiology of early and delayed injury after ICH is crucial to define potential targets of intervention and develop effective therapeutic strategies, in terms of neuroprotection.

PHE is not rare in ICH patients and is attributed to the secondary injury precipitated by the mechanical effects of expanding hematoma and toxic effects of blood degradation products on surrounding brain tissue (Lim-Hing and Rincon, 2017)**.**

PHE represents a radiological surrogate marker of secondary injury after ICH, considered as an epiphenomenon of ICH size and related to neurological deterioration, herniation, and death (Selim and Norton, 2020).

2*.2 Pathophysiology of perihematomal edema*

The formation and evolution of the PHE are characterized by a complex cascade of underlying heterogeneous events depending on the various developmental phases including: clot retraction with accumulation of electrolytes and serum under hydrostatic forces into the perihematomal space underlying the development of edema; thrombin formation; coagulation cascade; inflammation; Hemolysis of red blood cells (RBCs) and subsequent hemoglobin toxicity; complement activation; plasma protein leakage; and BBB disruption.

In the early stages the formation of edema is precipitated by the leakage of electrolytes and liquid from the damaged vessels and by the extravasation of plasma proteins and remodeling following the clot retraction. In the delayed phases PHE due to vasogenic edema is supported by BBB disruption and cytotoxic edema attributed to neuronal death, inflammation, and thrombin production and lysis of RBCs with release of hemoglobin-degradation products (i.e. iron) (Lim-Hing and Rincon, 2017). Hypoperfusion of the perihaemorrhagic area has been documented in ICH and may be associated with worse functional outcome, although the controversial role (Morotti et al., 2020).

Perihematomal hypoperfusion represents an epiphenomenon of perihematomal oedema evolution, such as an indirect consequence of growing oedema, independently associated with poor functional outcome (Morotti et al., 2022).

Another possible interpretation underlying the worse functional outcome associated with the development of perhematoma hypoperfusion is the finding of ischemic lesions as secondary irreversible damage, as supported by previous MRI studies (Boulanger et al., 2019; Yang et al., 2022)**.** However other studies have not confirmed the presence of penumbra, interpreting perihemorrhagic hypoperfusion as a likely consequence of reduced metabolic demand (diaschisis) rather than a sign of ischemia, consistent with positron emission tomography (PET) studies (Schellinger et al., 2003).

Some patients with ICH show lesions on diffusion-weighted (DW) magnetic resonance imaging (I) with a greater risk of unfavorable prognosis. Some studies have reported recurrence of ICH with DWI lesions. The relationship between mortality, ischemic stroke, and hematoma volume and DWI lesions is debated (Li et al., 2024).

DWI lesions after ICH, both in perihematomal region and remote region have been described. A presumed explanation may be due to decreased cerebral blood flow (CBF) around hematoma, and microvascular or bioenergetic compromise associated (Mayer et al., 1998). According to previous clinical studies, DWI lesions have also been attributed to ICH-mediated hypercoagulability and acute blood pressure fluctuations, but emerging evidence supports underlying cerebral small vessel disease

as hypothetical previous risk condition (Prabhakaran and Naidech, 2012), although the etiology and significance remain unclear.

A multi-hit model for development of secondary ischemic injury after ICH due to “Stroke-prone” state has been postulated, including aggressive BP-lowering, markers of microvasculopathy, and ICP elevation. In such patients, elevations of ICP, failure of autoregulation, and aggressive early BP-lowering could increase the risk of acute brain ischemia (Prabhakaran and Naidech, 2012).

2.3 Endothelin peptides

ET-1 is a potent vasoconstrictor 21-amino-acid long peptide, first isolated from the supernatant of cultured endothelial cells, belonging to a human endothelin family contains three 21-amino-acid long isopeptides, endothelin-1, endothelin-2 and endothelin-3 (ET-1, ET-2 and ET-3) (Yanagisawa et al., 1988). ET-1 is the major isopeptide of importance in the cardiovascular system, mainly producted by endothelial cells but also by a variety of other cell types including the inner medullary collecting duct and most other nephron segments, neurons of the central nervous system, postganglionic sympathetic neurons, and monocytes/macrophages. During pro-inflammatory conditions, vascular smooth muscle cells and pulmonary epithelial cells can reconvert to the production of ET-1. The existence of multiple endothelin receptor subtypes was postulated on the evidence of the characteristic biphasic blood pressure response to ET-1 in rats (Yanagisawa et al., 1988).

Both ETA and ETB receptors located on vascular smooth muscle mediate the potent vasoconstrictor effects.The ET_B receptor shows a dual role on vascular tone, as activation of ET_B receptors located on the endothelium stimulates the release of nitric oxide and vasodilator cyclooxygenase metabolites, with consequent vasorelaxant action on the underlying smooth muscle (Kedzierski and Yanagisawa, 2001).

The endothelin system has a basal vasoconstricting role and is involved in the development of diseases such as hypertension, atherosclerosis, and vasospasm after subarachnoid hemorrhage.Its potential role as an interesting therapeutic target in the treatment of a wide range of cardiovascular diseases is now known, as demonstrated by the non-selective antagonist, bosentan, currently used for the treatment of pulmonary arterial hypertension.

2.4 Nitric oxide

Nitric Oxide (NO) can be generated by three different isoforms of the enzyme NO synthase: Neuronal NOS (nNOS) is expressed in specific neurons of the central nervous system (CNS) and is involved in synaptic plasticity, in central control of blood pressure and atypical neurotransmission in the peripheral nervous system (PNS); Inducible NOS (iNOS) is produced by macrophages in response to cytokines and up-regulated during inflammation; Endothelial NOS-derived NO (eNOS) is a physiological vasodilator involved in vasoprotection and prevention of atherosclerosis (Forstermann and Sessa, 2012).

An abnormal production of nNOS has been implicated in N-methyl-d-aspartate receptor-mediated excitotossicity neuronal death after cerebrovascular stroke (Lipton et al., 1993).

During pro-inflammatory state, the high levels of NO produced by activated macrophages (and probably other cells) may not only be toxic to microbial pathogens and tumor cells but can damage the surrounding tissue (Forstermann and Sessa, 2012).

eNOS represents a homeostatic regulator of various essential cardiovascular functions, involved in vasodilatation and inhibition of platelet aggregation and adhesion (Radomski et al., 1987).

Therefore, under stressconditions, this molecule acts as a double-edged sword (Zhang et al., 2017).

In condition of brain hypoperfusion, the pro-oxidant activity exceeds the endogenous antioxidant defense leading to oxidative stress. Similarly to oxidative stress, nitrosative stress can occur due to the excessive production of nNOS derived reactive oxygen species (ROS) and of iNOS-derived NO,

which are responsible of protein, lipid and DNA damage leading to apoptosis and necrosis (Chen et al., 2009).

2.5 Asymmetric dimethyl-arginine (ADMA) and Nicotinamide adenine dinucleotide phosphate (NADPH)

ADMA is an endogenous inhibitor of NOS and is known to be a marker of endothelial disfunction and atherosclerosis. It seems to be involved in CBF reduction and in promoting oxidative stress and inflammatory response to ischemia (Won et al., 2011).

NADPH oxidase (NOX) is a complex multimeric enzyme that participates in the generation of superoxide or hydrogen peroxide (Gupta et al., 2020; Shah, 2007).

The NADPH oxidase/NOX enzyme system is the only known system whose main function is to release ROS. There are seven NOX subtypes: NOX1-5 and DUOX1/2 which differ for distribution, structure, and function (Haslund-Vinding et al., 2017).

In a rat model it was shown that NOX4 expression is upregulated after ICH, resulting in imbalance in the oxidative stress, leading to apoptosis and disruption of the BBB due to secondary brain injury (SBI) following ICH (Xie et al., 2020).

2.6 Oxidative stress after ICH

Oxidative stress exhibits a key role in the development of secondary brain injury (SBI) after ICH, as well as inflammatory response, mitochondrial dysfunction, and cell death.

After heme is decomposed in the degradation product of hemoglobin, the consequent excess iron determines mitochondrial dysfunction and produces oxidative damage. In the meanwhile, highly reactive toxic radicals are produced during the reaction, resulting in lipid peroxidation, and excitotoxicity (Shao et al., 2022).

Another source of reactive oxygen species (ROS) after ICH depends on inflammatory response.

The pro-inflammatory M1 phenotype of Microglia predominance derived from M2 to M1 shift results in accumulation of ROS and a high production of pro-inflammatory factors.

In a normal homeostatic balance ROS can be neutralized trough antioxidant agents until this dynamic balance is compromised by the accumulation of ROS in excess, resulting in macromolecular damage, impaired cell signaling, cell death, and tissue damage, which can lead to further SBI (Forrester et al., 2018).

The relationship between oxidative stress and SBI after ICH represents a challenge for scientific research for the purpose of a better understanding of the pathophysiology of ICH with evident implications for clinical practice in terms of potential therapeutic targets.

2.7 Aim of the study

Main aim of this study was to assess the role of vasoactive substances (ET1 and NO), oxidative stress markers (ADMA and NOX2) in the development of perihematomal hypoperfusion and ischemic lesions.

Secondly, we aimed to study the correlation between these molecular biomarkers and the evolution of hematoma and perilesional edema volume.

Finally, we evaluated the impact of these variables on clinical outcome.

3. MATERIAL AND METHODS

3.1 Patients

In this study, we included patients with spontaneous ICH, admitted to the Emergency Department of our hospital, within 6 hours of symptom onset, between January 2019 and July 2021. For each patient we collected demographic data, pre-stroke modified Rankin Scale (mRS), vascular risk factors, previous medical therapy, presence of infections in the previous two weeks, stressful factors at the time of the event. We defined three time points from symptom onset for the collection of clinical and diagnostic data: time 0, at admission (T0); time 1 (T1) at 12-24h and time 2 (T2) at 48-72h. At T0, we performed general and neurological examination, measurement of vital parameters (blood pressure, heart rate and body temperature) and of serum glucose, assessment of stroke severity by using the National Institutes of Health Stroke Scale (NIHSS) score and plain brain Computed Tomography (CT) scan. We took blood samples at the three prespecified timepoints for the routine blood tests and for dosing the following molecular biomarkers: ET-1, NO, sNOX2-dp, ADMA as described below. The T0 sampling was collected prior to the administration of any drug. At T1, we performed a brain Magnetic Resonance Imaging (MRI) including diffusion (DW) and perfusion (PW) weighted images, clinical evaluation with NIHSS and blood pressure measurement. At T2, we undertook a follow-up MRI (DWI), Apparent diffusion coefficient (ADC) map, Fluid attenuated inversion recovery (FLAIR) and Gradient Echo (GE).

Finally, we evaluated the level of disability at 3 months after the acute event using the modified Rankin scale (mRS) by telephone interview (T3). A schematic representation of the study experimental design is depicted in Figure 1.

All study participants gave a written informed consent. The study was approved by the Ethical Committee of the Policlinico Umberto I University Hospital (number 5875) and was conducted according to the Declaration of Helsinki.

3.2 Laboratory data

Blood samples obtained from patients were collected into tubes with or without anticoagulant (with 3.8% sodium citrate) and centrifuged at 300 g for 10 min at room temperature, to obtain supernatant. Plasma and serum samples were immediately stored at −80 °C until the time of analysis.

3.3. sNOX2-dp, ADMA, ET-1

Serum NOX2 were measured as sNOX2-dp with an ELISA method as previously reported[23]. Values were expressed as pg/ml; intra-assay and inter-assay coefficients of variation were 8.95% and 9.01%, respectively.

Quantitative determination of ADMA and ET-1 levels was measured in serum samples by ELISA kit according to manufacture instructions. The values for ADMA were expressed in ng/mL and for ET-1 in pg/mL. Both intra- and inter-assay coefficients of variation were <10%

3.4. Nitric Oxide (NO) Assay

NO production was evaluated in the serum samples. A colorimetric assay kit (Abcam, Cambridge, UK) was used to determine the metabolites of NO (nitrites and nitrates, NOx) in 100 µL of samples under stirring conditions for 10 min at 37 °C. Values are expressed as µM. Intra-a and inter-assay coefficients of variation were 2.9% and 1.7%, respectively.

3.5. Radiological data

Two independent investigators used the ABC/2 formula to calculate the hematoma volume. At CT images, we applied the ABC/2 formula to the hemorrhagic lesion visible as hyperdensity (+ 30-45 Hounsfield unit, HU). At MRI images, we applied the formula to the visible hypointensity in the GRE sequence, while for the calculation of the edema volume the score was applied to the visible hyperintensity in the FLAIR sequence. Perihematomal edema volume was measured by subtracting the hematoma volume from the combined hematoma and perihematomal hyperintensity area volumes. Perihematomal edema was considered mild if only sulci effacement was present, moderate in the presence of ventricle asymmetry, and severe if there was midline shift. The midline shift (mm) was also measured. We also took into consideration the hematoma growth defined as any volume change from T1 to T2. The "island sign", defined as ≥3 small discrete hematomas that are not connected to the primary hematoma or ≥4 small hematomas that may branch off from the primary hematoma and resemble "bubbles" or "sprouts" rather than a lobulated appearance, was evaluated at the basal brain CT. Finally, we considered Mean Transit Time (MTT), Cerebral Blood Flow (CBF), and Cerebral Blood Volume (CBV), for the evaluation of hypoperfusion related to the hemorrhagic lesion. We measured CBF, CBV, and MTT values in 5 round regions of interest of about 0.5 cm^2 within 1 cm from the hematoma periphery and drawn freehand on the slice in which the hemorrhage was more visible. Values were averaged and expressed as continuous and categorical variables. According to previously published paper (Fainardi et al., 2008), CBF was categorized into normal (40–55 mL/100 g/min) and low (<40 mL/100 g/min); CBV was dichotomized into normal (>2.5 mL/100 g) and low (≤2.5 mL/100 g) and MTT was dichotomized into normal (≤5 s) and high (>5 s).

According to the results from MRI images, we divided the patients in two groups: patients with the presence of one or more ischemic lesions in the diffusion sequences at T1 and patients without ischemic lesions at T1.

3.6 Statistical analysis

The descriptive statistical analysis of the total population and of the two groups of interest was carried out by calculating means or medians for continuous variables based on their normal or non-normal distribution as well as by calculating frequencies, proportions (or percentages) for dichotomic/categorical variables. For comparison between the two groups of patients with ischemic lesions and patients without ischemic lesions: continuous variables with normal and non-normal distributions were compared using the t-test for paired samples or the Mann-Whitney U-test, respectively. We compared categorical variables using the Fisher test or chi-square test, when appropriate. Correlations between variables were assessed by calculating the Pearson or Spearman coefficient. We presented the course of the molecular biomarkers across the different time points, as well as the median changes over time by presence/absence of ischemic lesions at T1. Given the small numbers of patients included in the study, we performed an exploratory multivariate logistic regression to detect potential predictors of the development of perihematomal ischemic lesions after adjustment for age, sex and variables with a univariate p value <0.05. For all tests that were performed, a value of $p<0.05$ was considered statistically significant. Statistical analysis was performed using SPSS statistical software (IBM Corp, SPSS Statistics for Windows, Version 25, Armonk, NY).

4. RESULTS

We enrolled 28 patients with ICH, 15 males (55.2%) and 13 females (44.8%), mean (± SD) age 70.2 years (± 13.8). Pre-stroke mRS was between 0 and 1 in 24 (85.2%) patients. Overall, 12 patients (42.8%) had one or more ischemic lesions in DW-MRI at T1, while there were 16 patients (57.1%) without ischemic lesions.

4.1. Patients' characteristics

We did not find any statistically significant differences between the two groups as regards demographic characteristics and NIHSS score, blood pressure, heart rate and serum glucose values at the three assessment timepoints (Table 1 and Table 2). However, we found a higher prevalence of past medical history of hypertension (12 [100%] vs 9 [56.3%] patients; p= 0.010) and of dyslipidemia (9 [75%] patients vs 1 [6.3%] patient, p<0.001) and a higher prevalence of neutrophil leukocyte counts at T0 (7.44 $x10^3/\mu L$ vs 4.99 $x10^3/\mu L$; p <0.037) in the group of patients with ischemic lesions.

4.2. Radiological features

Patients with ischemic lesions (Figure 2) had a median hematoma volume at T1 significantly larger than that of patients without ischemic lesions (23.05 cm3 vs 6.65 cm3, p<0.005) and a significantly higher volume of perilesional edema (15.25 vs 8.25 cm3, p 0.046) with a more severe midline shift [4.45 mm (±4.74) vs 1.31 mm (±2.62) (p=0.036)] (Supplemental Table 1). This data was also confirmed at T2 (Supplemental Table 1). The "island sign" was more frequently observed in group 1 (10 [83.3%] vs 4/15 patients [26.7%], p 0.003). When associations between prespecified perfusion parameters and the development of ischemic lesions at T1 or T2 were investigated, we did not find statistically significant differences.

4.3. Clinical outcomes

No statistically significant between-group differences were found in terms of functional outcome at 3 months, intra-hospital death, and mortality at 3 months (Supplementary Table 2).

4.4. Serum biomarkers

Patients with ischemic lesions at T1 showed a higher median serum concentration of sNOX2-dp at T0 compared to those without ischemic lesions, although the difference had a borderline statistical significance (34.9 pg/ml vs 22.4 pg/ml, p=0.051). (Figure 3 and Supplementary Table 3).

For the remaining serum biomarkers, no statistically significant differences were found between the two groups at the three time points (Supplementary Table 3 and Supplementary Figure 1).

In the exploratory multivariate analysis, after adjustment for age, sex, neutrophil absolute number at T0 and hematoma volume at T1, high sNOX2-dp values at T0 were associated with the development of perihematomal ischemic lesions at T1, although with a trend toward the statistical significance (OR 1.122, 95% CI 0.991-1.269, p: 0.068). Changes of biomarker levels from a timepoint to another in the two groups are summarized in Supplementary Table 4 and Supplementary Figure 2.

4.5. Association between serum biomarkers and radiological characteristics of hematoma and clinical outcome

Higher levels of ET-1 at T1 significantly correlated with smaller hematoma volumes at T2 (Spearman's rho= -0.717, p=0.030) with only a trend toward the statistical significance for ET-1 levels at T0 (Spearman's rho= -0.617, p=0.077) (Figure 4).

Consistently, patients without any hematoma growth from T1 to T2 had higher levels of ET-1 at T2 compared with those with any hematoma growth (16.70 pg/ml vs. 12.83 pg/ml, p=0.020) (Figure 5).

Higher levels of ET-1 at T1 were also associated with a borderline statistically significant absence of ipsilateral hemispheric hypoperfusion at T1 (17.76 pg/ml vs. 11.54 pg/ml, p=0.059 (Supplementary Figure 3).

Patients with a more severe perihematomal edema at T2 had higher levels of sNOX2-dp at T0 (37.99 pg/ml vs. 19.17 pg/ml, p=0.011) and of NO at T2 (32.64 μM vs. 14.03 μM, p=0.039) (Supplementary Figure 4).

A significant linear positive correlation was found between high levels of some biomarkers and neurological severity measured by NIHSS score at different timepoints, such as NO at T1 (Spearman's rho=0.783, p=0.007) with NIHSS at discharge T1, while there was an inverse correlation between ADMA levels at T2 and NIHSS at T2 (Spearman's rho= -0.743, p=0.009) (Supplementary Figure 5).

We did not find any statistically significant association between levels of biomarkers at any timepoint and intra-hospital mortality or clinical outcome at 3 months measured by mRS score (Supplementary Figures 6 and 7). Patients with high levels of NO at T0 (28.86 vs 8.69 in the survivors, p=0.035) were more likely to die at 3 months (Supplementary Figure 8).

5. DISCUSSION

In this study, we aimed to identify biological markers potentially involved in the development of secondary brain injury following ICH, specifically focusing on perihematomal hypoperfusion, ischemic lesions, hematoma expansion, and edema development.

The pathophysiology of ICH is still not fully understood. Beyond the initial phase, where extravasated blood causes mechanical disruption of brain structures and increased intracranial pressure, a second phase follows. This phase is characterized by hematoma expansion and the development of vasogenic edema due to the rupture of the blood-brain barrier (BBB) (Wilkinson et al., 2018). A complex series of events occurs during this phase, involving hemoglobin, iron, hemin, and thrombin toxicity. These factors contribute to the disruption of the endothelium and tight junctions, leading to inflammatory cell invasion, increased calcium and free radical production, extensive microglia activation, and ultimately, increased neuronal death and axonal damage (Bautista et al., 2021)

Our study found that approximately 42% of ICH patients developed ischemic damage within 48-72 hours after onset, consistent with previous studies (Li et al., 2013). Although patients with ischemic perihematomal lesions had higher sNOX2-dp levels at admission compared to those without lesions, this difference did not reach statistical significance likely due to our small sample size. However, sNOX2-dp levels were significantly associated with the development of severe edema at 72 hours. While no significant correlation was observed between ischemic lesions and worse outcomes as measured by the mRS at three months, we found a significant association between ischemic lesions and any increase of hematoma volume, perilesional edema, and greater midline shift. These findings suggest that oxidative stress, indicated by sNOX2-dp levels, plays a key role in the development of ischemic perihematomal lesions, aligning with previous research indicating that oxidative stress contributes to secondary brain injury in ICH (Bautista et al., 2021; Boulanger et al., 2019; Fainardi et al., 2008; Wilkinson et al., 2018; Yang et al., 2022).

It is important to note that our measurements were based on plasma nitrites/nitrates as surrogate markers for NO, which do not distinguish between NO produced by eNOS, nNOS, or iNOS. While eNOS-derived NO is generally considered neuroprotective in cerebral ischemia 33-34 due to its vasodilatory and anti-inflammatory effects, excessive NO production from nNOS or iNOS could lead to nitrosative stress, resulting in damage to proteins, lipids, and DNA in ICH, thereby worsening outcomes. Consistent with this hypothesis, we found a significant inverse correlation between the levels of the endogenous NOS inhibitor ADMA at T2 and NIHSS scores at T2.

Furthermore, in response to sNOX2-dp activation, we observed a decrease of ET-1 levels. Since the increased formation of superoxide anions by sNOX2-dp activation promotes ET-1 reduction in the endothelium (Kamhieh-Milz et al., 2023) suggesting a putative link between the sNOX2-dp activation and ET-1 expression, we speculated that the reduction of ET-1 levels in the endothelium might represent a compensatory response to modulate and counteract the oxidative stress and endothelial dysfunction observed in this context.

In fact, our results showed an inverse correlation between ET-1 levels at 12-24 hours and hemorrhage volume at 48-72 hours. This suggests that ET-1 may exert a protective effect by inducing vasoconstriction of the ruptured vessel, limiting hematoma expansion. ET-1 is a powerful vasoconstrictor locally released by the endothelium at the site of vessel injury, initiating vasospasm as the first step in primary hemostasis, potentially leading to the cessation of bleeding (Periayah et al., 2017). In our study, patients with higher ET-1 plasma levels exhibited less hematoma growth and did not develop ischemic damage. This suggests that ET-1 might induce vasoconstriction in the damaged artery responsible for the bleeding, thereby reducing blood supply to the injured area and preventing hematoma expansion. This reduction in hematoma growth may protect the surrounding parenchyma and prevent the development of ischemic perihematomal lesions. These findings contradict those of Alioglu et al (Alioğlu et al., 2000), who reported that higher ET-1 levels were associated with increased hematoma volume and worse prognosis. To the best of our knowledge, the study by Alioglu's group is the only one in the literature that addresses the potential role of ET-1 in

patients with ICH. Most research has focused on the role of ET-1 in ischemic stroke and subarachnoid hemorrhage. In ischemic stroke, an acute increase in ET-1 plasma levels has been associated with cerebral vasoconstriction, reduced regional blood flow and microcirculation, and larger infarct volumes (Alioglu et al., 2002; Sapira et al., 2010; Ziv et al., 1992). Additionally, animal studies on subarachnoid hemorrhage have demonstrated that ET-1 administration into cerebrospinal fluid can induce severe vasospasm (Bertsch et al., 2001; Davenport et al., 2016; Faßbender et al., 2000)

The discrepancy between the findings on ET-1 levels in our study and Alioglu et al.'s study likely results from a combination of factors, including differences in study design, timing and methodology of ET-1 measurement, patient populations, severity of ICH, clinical outcome measurement tools and follow-up times. A more detailed exploration of these variables in future studies could help to clarify the role of ET-1 in ICH and resolve these discrepancies. It is also possible that ET-1 exerts different actions depending on the timing of the bleeding onset. The vasoconstrictor effect may be beneficial at the beginning of the bleeding process, but it could become harmful in later phases when reduced blood flow might cause surrounding hypoperfusion and perihematomal damage. Moreover, the endothelin system is very complex, and its effects can vary depending on the receptors activated: stimulation of the ET_A receptor induces potent and prolonged vasoconstriction, inflammation, and cell proliferation, whereas stimulation of the ET_B receptor generally produces the opposite effects (Davenport et al., 2016).

Furthermore, from the overall analysis of the patients it emerged that the values of

ET-1 are higher in both patient subgroups as compared to those reported in the literature of healthy subjects (0.1 and 5.0 fmol/mL.) 119, with an increase in the early stages and a decreasing trend until T2. This trend could be due to increased clearance of the molecule or to its binding with subsequent internalization of the receptor and consequent decrease in plasma free ET-1 values. After ischemic brain injury, for example, an increase in plasticity was found in terms of an up-regulation, especially of the receptors ET B, in the expression of the smooth muscle cells of downstream arteries and arterioles of vessel occlusion.

To confirm the role of vasoconstriction as compensatory response to oxidative stress condition we also evaluated ADMA levels that is an endogenous inhibitor of NO-synthase and its elevated concentrations in the blood are found in numerous diseases associated with endothelial dysfunction (Valkonen et al., 2003). Moreover, it was demonstrated that ADMA activates the local renin-angiotensin system, and the angiotensin II released activates NAD(P)H oxidase; superoxide produced interferes with the bioavailability of NO, resulting in diminished flow-induced dilation, a mechanism that may contribute to the development of endothelial dysfunction increasing tone associated with elevated ADMA levels (Luo et al., 2010). We found that ADMA levels decreased at T1 and T2 in comparison with T0 and we also found a significant inverse correlation between the levels of ADMA and NIHSS scores at T2. These results corroborate with our hypothesis that a reduction of the bioavailability of NO and consequently reduction of NO-mediated dilations is countered by compensatory mechanisms such as reduction of ET-1 and ADMA levels.

The primary limitation of our study is the small sample size, which may have limited our ability to detect statistically significant differences for some biomarkers. Additionally, the complexity of the study design and the use of surrogate markers for NO production could affect the interpretation of our findings.

The strengths of this study lie in its comprehensive biomarker analysis, integration of advanced imaging techniques, focus on clinically relevant outcomes, exploration of understudied biomarkers, and its prospective design.

In conclusion, our study suggests that sNOX2-dp is linked to the development of ischemic perihematomal lesions, while ET-1 may help to limit hematoma expansion by inducing vasoconstriction of the bleeding artery. Conversely, NO appears to be associated with worse outcomes and increased mortality, likely due to its role in free radical production. Larger, prospective studies are needed to confirm these findings and further clarify the roles of these biomarkers in ICH, ultimately aiming to develop targeted therapeutic strategies to improve patient outcomes.

6. CONCLUSIONS

ICH still represents one of the main causes of death and disability in the general population and especially in developing countries development. Despite the considerable progress achieved in the medical field in the last twenty years, in particular in ischemic stroke, the resources therapies to counteract this pathology and improve the quality of life of patients and reduce mortality, are still not satisfactory.

Recently there has been an increased interest on the pathophysiological mechanisms underlying hemorrhage and perilesional damage. Although the role of ischemic injury potentially involving the surrounding parenchyma during ICH remains not completely clarified by experimental studies, in the future the confirmation of this data with potential intervention strategies on the rescue of the so-called penumbra could represent an interesting challenge of research to carry forward.

ET-1 could play a decisive role, as potent vasoconstrictor, resulting in stemming the expansion of the hematoma and sNOX2-dp seems to be involved in the development of ischemic perihematomal injury.

Understanding the mechanisms underlying the expansion of hemorrhage and the identification of biochemical and radiological markers that can improve the evaluation of the prognosis of these patients still represents an open challenge.

Present data, although preliminary, offer starting points for future research aimed at understanding the underlying pathophysiological mechanisms of the expansion of the cerebral hemorrhage and, if confirmed on larger population sample, could subsequently provide the basis for specific pharmacological targets.

7. REFERENCES

Alioğlu, Z., Bülbül, I., Örem, A., Özmenoğlu, M., Vanizor, B., Boz, C., 2000. Increased plasma endothelin-1 levels in patients with intracerebral hemorrhage. J. Stroke Cerebrovasc. Dis. 9, 176–180. https://doi.org/10.1053/jscd.2000.7231

Alioglu, Z., Örem, A., Bülbül, I., Boz, C., Özmenoğlu, M., Vanizor, B., 2002. Evaluation of Plasma Endothelin-1 Levels in Patients with Cerebral Infarction. Angiology 53, 77–82. https://doi.org/10.1177/000331970205300110

Bautista, W., Adelson, P.D., Bicher, N., Themistocleous, M., Tsivgoulis, G., Chang, J.J., 2021. Secondary mechanisms of injury and viable pathophysiological targets in intracerebral hemorrhage. Ther. Adv. Neurol. Disord. 14, 17562864211049208. https://doi.org/10.1177/17562864211049208

Bertsch, T., Kuehl, S., Muehlhauser, F., Walter, S., Hodapp, B., Rossol, S., Schmeck, J., Ragoschke, A., Schütt, S., Fritzinger, M., Horn, P., Vajkoczy, P., Wendel-Wellner, M., Faßbender, K., 2001. Source of Endothelin-1 in Subarachnoid Hemorraghe. Clin. Chem. Lab. Med. 39. https://doi.org/10.1515/CCLM.2001.053

Boulanger, M., Schneckenburger, R., Join-Lambert, C., Werring, D.J., Wilson, D., Hodel, J., Zuber, M., Touzé, E., 2019. Diffusion-Weighted Imaging Hyperintensities in Subtypes of Acute Intracerebral Hemorrhage: Meta-Analysis. Stroke 50, 135–142. https://doi.org/10.1161/STROKEAHA.118.021407

Chen, H., Song, Y.S., Chan, P.H., 2009. Inhibition of NADPH Oxidase is Neuroprotective after Ischemia—Reperfusion. J. Cereb. Blood Flow Metab. 29, 1262–1272. https://doi.org/10.1038/jcbfm.2009.47

Davenport, A.P., Hyndman, K.A., Dhaun, N., Southan, C., Kohan, D.E., Pollock, J.S., Pollock, D.M., Webb, D.J., Maguire, J.J., 2016. Endothelin. Pharmacol. Rev. 68, 357–418. https://doi.org/10.1124/pr.115.011833

Fainardi, E., Borrelli, M., Saletti, A., Schivalocchi, R., Azzini, C., Cavallo, M., Ceruti, S., Tamarozzi, R., Chieregato, A., 2008. CT perfusion mapping of hemodynamic disturbances associated to acute spontaneous intracerebral hemorrhage. Neuroradiology 50, 729–740. https://doi.org/10.1007/s00234-008-0402-x

Faßbender, K., Hodapp, B., Rossol, S., Bertsch, T., Schmeck, J., Schütt, S., Fritzinger, M., Horn, P., Vajkoczy, P., Wendel-Wellner, M., Ragoschke, A., Kuehl, S., Brunner, J., Schürer, L., Schmiedeck, P., Hennerici, M., 2000. Endothelin-1 in Subarachnoid Hemorrhage: An Acute-Phase Reactant Produced by Cerebrospinal Fluid Leukocytes. Stroke 31, 2971–2975. https://doi.org/10.1161/01.STR.31.12.2971

Feigin, V.L., Stark, B.A., Johnson, C.O., Roth, G.A., Bisignano, C., Abady, G.G., Abbasifard, M., Abbasi-Kangevari, M., Abd-Allah, F., Abedi, V., Abualhasan, A., Abu-Rmeileh, N.M., Abushouk, A.I., Adebayo, O.M., Agarwal, G., Agasthi, P., Ahinkorah, B.O., Ahmad, S., Ahmadi, S., Ahmed Salih, Y., Aji, B., Akbarpour, S., Akinyemi, R.O., Al Hamad, H., Alahdab, F., Alif, S.M., Alipour, V., Aljunid, S.M., Almustanyir, S., Al-Raddadi, R.M., Al-Shahi Salman, R., Alvis-Guzman, N., Ancuceanu, R., Anderlini, D., Anderson, J.A., Ansar, A., Antonazzo, I.C., Arabloo, J., Ärnlöv, J., Artanti, K.D., Aryan, Z., Asgari, S., Ashraf, T., Athar, M., Atreya, A., Ausloos, M., Baig, A.A., Baltatu, O.C., Banach, M., Barboza, M.A., Barker-Collo, S.L., Bärnighausen, T.W., Barone, M.T.U., Basu, S., Bazmandegan, G., Beghi, E., Beheshti, M., Béjot, Y., Bell, A.W., Bennett, D.A., Bensenor, I.M., Bezabhe, W.M., Bezabih, Y.M., Bhagavathula, A.S., Bhardwaj, P., Bhattacharyya, K., Bijani, A., Bikbov, B., Birhanu, M.M., Boloor, A., Bonny, A., Brauer, M., Brenner, H., Bryazka, D., Butt, Z.A., Caetano Dos Santos, F.L., Campos-Nonato, I.R., Cantu-Brito, C., Carrero, J.J., Castañeda-Orjuela, C.A., Catapano, A.L., Chakraborty, P.A., Charan, J., Choudhari, S.G., Chowdhury, E.K., Chu, D.-T., Chung, S.-C., Colozza, D., Costa, V.M., Costanzo, S., Criqui, M.H., Dadras, O., Dagnew, B., Dai, X., Dalal, K., Damasceno, A.A.M., D'Amico, E., Dandona, L., Dandona, R., Darega Gela, J., Davletov, K., De La Cruz-Góngora, V., Desai, R., Dhamnetiya, D., Dharmaratne,

S.D., Dhimal, M.L., Dhimal, M., Diaz, D., Dichgans, M., Dokova, K., Doshi, R., Douiri, A., Duncan, B.B., Eftekharzadeh, S., Ekholuenetale, M., El Nahas, N., Elgendy, I.Y., Elhadi, M., El-Jaafary, S.I., Endres, M., Endries, A.Y., Erku, D.A., Faraon, E.J.A., Farooque, U., Farzadfar, F., Feroze, A.H., Filip, I., Fischer, F., Flood, D., Gad, M.M., Gaidhane, S., Ghanei Gheshlagh, R., Ghashghaee, A., Ghith, N., Ghozali, G., Ghozy, S., Gialluisi, A., Giampaoli, S., Gilani, S.A., Gill, P.S., Gnedovskaya, E.V., Golechha, M., Goulart, A.C., Guo, Y., Gupta, R., Gupta, V.B., Gupta, V.K., Gyanwali, P., Hafezi-Nejad, N., Hamidi, S., Hanif, A., Hankey, G.J., Hargono, A., Hashi, A., Hassan, T.S., Hassen, H.Y., Havmoeller, R.J., Hay, S.I., Hayat, K., Hegazy, M.I., Herteliu, C., Holla, R., Hostiuc, S., Househ, M., Huang, J., Humayun, A., Hwang, B.-F., Iacoviello, L., Iavicoli, I., Ibitoye, S.E., Ilesanmi, O.S., Ilic, I.M., Ilic, M.D., Iqbal, U., Irvani, S.S.N., Islam, S.M.S., Ismail, N.E., Iso, H., Isola, G., Iwagami, M., Jacob, L., Jain, V., Jang, S.-I., Jayapal, S.K., Jayaram, S., Jayawardena, R., Jeemon, P., Jha, R.P., Johnson, W.D., Jonas, J.B., Joseph, N., Jozwiak, J.J., Jürisson, M., Kalani, R., Kalhor, R., Kalkonde, Y., Kamath, A., Kamiab, Z., Kanchan, T., Kandel, H., Karch, A., Katoto, P.D., Kayode, G.A., Keshavarz, P., Khader, Y.S., Khan, E.A., Khan, I.A., Khan, M., Khan, M.A., Khatib, M.N., Khubchandani, J., Kim, G.R., Kim, M.S., Kim, Y.J., Kisa, A., Kisa, S., Kivimäki, M., Kolte, D., Koolivand, A., Koulmane Laxminarayana, S.L., Koyanagi, A., Krishan, K., Krishnamoorthy, V., Krishnamurthi, R.V., Kumar, G.A., Kusuma, D., La Vecchia, C., Lacey, B., Lak, H.M., Lallukka, T., Lasrado, S., Lavados, P.M., Leonardi, M., Li, B., Li, S., Lin, H., Lin, R.-T., Liu, X., Lo, W.D., Lorkowski, S., Lucchetti, G., Lutzky Saute, R., Magdy Abd El Razek, H., Magnani, F.G., Mahajan, P.B., Majeed, A., Makki, A., Malekzadeh, R., Malik, A.A., Manafi, N., Mansournia, M.A., Mantovani, L.G., Martini, S., Mazzaglia, G., Mehndiratta, M.M., Menezes, R.G., Meretoja, A., Mersha, A.G., Miao Jonasson, J., Miazgowski, B., Miazgowski, T., Michalek, I.M., Mirrakhimov, E.M., Mohammad, Y., Mohammadian-Hafshejani, A., Mohammed, S., Mokdad, A.H., Mokhayeri, Y., Molokhia, M., Moni, M.A., Montasir, A.A., Moradzadeh, R., Morawska, L., Morze, J., Muruet, W., Musa,

K.I., Nagarajan, A.J., Naghavi, M., Narasimha Swamy, S., Nascimento, B.R., Negoi, R.I., Neupane Kandel, S., Nguyen, T.H., Norrving, B., Noubiap, J.J., Nwatah, V.E., Oancea, B., Odukoya, O.O., Olagunju, A.T., Orru, H., Owolabi, M.O., Padubidri, J.R., Pana, A., Parekh, T., Park, E.-C., Pashazadeh Kan, F., Pathak, M., Peres, M.F.P., Perianayagam, A., Pham, T.-M., Piradov, M.A., Podder, V., Polinder, S., Postma, M.J., Pourshams, A., Radfar, A., Rafiei, A., Raggi, A., Rahim, F., Rahimi-Movaghar, V., Rahman, M., Rahman, M.A., Rahmani, A.M., Rajai, N., Ranasinghe, P., Rao, C.R., Rao, S.J., Rathi, P., Rawaf, D.L., Rawaf, S., Reitsma, M.B., Renjith, V., Renzaho, A.M.N., Rezapour, A., Rodriguez, J.A.B., Roever, L., Romoli, M., Rynkiewicz, A., Sacco, S., Sadeghi, M., Saeedi Moghaddam, S., Sahebkar, A., Saif-Ur-Rahman, K., Salah, R., Samaei, M., Samy, A.M., Santos, I.S., Santric-Milicevic, M.M., Sarrafzadegan, N., Sathian, B., Sattin, D., Schiavolin, S., Schlaich, M.P., Schmidt, M.I., Schutte, A.E., Sepanlou, S.G., Seylani, A., Sha, F., Shahabi, S., Shaikh, M.A., Shannawaz, M., Shawon, M.S.R., Sheikh, A., Sheikhbahaei, S., Shibuya, K., Siabani, S., Silva, D.A.S., Singh, J.A., Singh, J.K., Skryabin, V.Y., Skryabina, A.A., Sobaih, B.H., Stortecky, S., Stranges, S., Tadesse, E.G., Tarigan, I.U., Temsah, M.-H., Teuschl, Y., Thrift, A.G., Tonelli, M., Tovani-Palone, M.R., Tran, B.X., Tripathi, M., Tsegaye, G.W., Ullah, A., Unim, B., Unnikrishnan, B., Vakilian, A., Valadan Tahbaz, S., Vasankari, T.J., Venketasubramanian, N., Vervoort, D., Vo, B., Volovici, V., Vosoughi, K., Vu, G.T., Vu, L.G., Wafa, H.A., Waheed, Y., Wang, Y., Wijeratne, T., Winkler, A.S., Wolfe, C.D.A., Woodward, M., Wu, J.H., Wulf Hanson, S., Xu, X., Yadav, L., Yadollahpour, A., Yahyazadeh Jabbari, S.H., Yamagishi, K., Yatsuya, H., Yonemoto, N., Yu, C., Yunusa, I., Zaman, M.S., Zaman, S.B., Zamanian, M., Zand, R., Zandifar, A., Zastrozhin, M.S., Zastrozhina, A., Zhang, Y., Zhang, Z.-J., Zhong, C., Zuniga, Y.M.H., Murray, C.J.L., 2021. Global, regional, and national burden of stroke and its risk factors, 1990–2019: a systematic analysis for the Global Burden of Disease Study 2019. Lancet Neurol. 20, 795–820. https://doi.org/10.1016/S1474-4422(21)00252-0

Flaherty, M.L., Haverbusch, M., Sekar, P., Kissela, B., Kleindorfer, D., Moomaw, C.J., Sauerbeck, L., Schneider, A., Broderick, J.P., Woo, D., 2006. Long-term mortality after intracerebral hemorrhage. Neurology 66, 1182–1186. https://doi.org/10.1212/01.wnl.0000208400.08722.7c

Forrester, S.J., Kikuchi, D.S., Hernandes, M.S., Xu, Q., Griendling, K.K., 2018. Reactive Oxygen Species in Metabolic and Inflammatory Signaling. Circ. Res. 122, 877–902. https://doi.org/10.1161/CIRCRESAHA.117.311401

Forstermann, U., Sessa, W.C., 2012. Nitric oxide synthases: regulation and function. Eur. Heart J. 33, 829–837. https://doi.org/10.1093/eurheartj/ehr304

Gupta, R.M., Libby, P., Barton, M., 2020. Linking regulation of nitric oxide to endothelin-1: The Yin and Yang of vascular tone in the atherosclerotic plaque. Atherosclerosis 292, 201–203. https://doi.org/10.1016/j.atherosclerosis.2019.11.001

Haslund-Vinding, J., McBean, G., Jaquet, V., Vilhardt, F., 2017. NADPH oxidases in oxidant production by microglia: activating receptors, pharmacology and association with disease. Br. J. Pharmacol. 174, 1733–1749. https://doi.org/10.1111/bph.13425

Jolink, W.M.T., Klijn, C.J.M., Brouwers, P.J.A.M., Kappelle, L.J., Vaartjes, I., 2015. Time trends in incidence, case fatality, and mortality of intracerebral hemorrhage. Neurology 85, 1318–1324. https://doi.org/10.1212/WNL.0000000000002015

Kamhieh-Milz, J., Chen, L., Goettsch, C., Pfefferkorn, A.M., Hofmann, A., Brunssen, C., Müller, G.M., Walther, T., Ashraf, M.I., Moll, G., Morawietz, H., Witowski, J., Catar, R., 2023. Ang II Promotes ET-1 Production by Regulating NOX2 Activity Through Transcription Factor Oct-1. Arterioscler. Thromb. Vasc. Biol. 43, 1429–1440. https://doi.org/10.1161/ATVBAHA.122.318764

Kedzierski, R.M., Yanagisawa, M., 2001. Endothelin System: The Double-Edged Sword in Health and Disease. Annu. Rev. Pharmacol. Toxicol. 41, 851–876. https://doi.org/10.1146/annurev.pharmtox.41.1.851

Lattanzi, S., Di Napoli, M., Ricci, S., Divani, A.A., 2020. Matrix Metalloproteinases in Acute Intracerebral Hemorrhage. Neurotherapeutics 17, 484–496. https://doi.org/10.1007/s13311-020-00839-0

Li, N., Worthmann, H., Heeren, M., Schuppner, R., Deb-Chatterji, M., Tryc, A.B., Bueltmann, E., Lanfermann, H., Donnerstag, F., Weissenborn, K., Raab, P., 2013. Temporal Pattern of Cytotoxic Edema in the Perihematomal Region After Intracerebral Hemorrhage: A Serial Magnetic Resonance Imaging Study. Stroke 44, 1144–1146. https://doi.org/10.1161/STROKEAHA.111.000056

Li, Y., Lei, C., Wang, L., Lin, S., Zhao, L., Jiang, W., Deng, Q., Yang, X., 2024. Systematic Review and Meta-Analysis of the Association Between Appearance of Lesions on Diffusion-Weighted Imaging and Poor Outcomes Among Patients with Intracerebral Hemorrhage. World Neurosurg. 190, 323–328. https://doi.org/10.1016/j.wneu.2024.07.168

Lim-Hing, K., Rincon, F., 2017. Secondary Hematoma Expansion and Perihemorrhagic Edema after Intracerebral Hemorrhage: From Bench Work to Practical Aspects. Front. Neurol. 8. https://doi.org/10.3389/fneur.2017.00074

Lipton, S.A., Choi, Y.-B., Pan, Z.-H., Lei, S.Z., Chen, H.-S.V., Sucher, N.J., Loscalzo, J., Singel, D.J., Stamler, J.S., 1993. A redox-based mechanism for the neuroprotective and neurodestructive effects of nitric oxide and related nitroso-compounds. Nature 364, 626–632. https://doi.org/10.1038/364626a0

Luo, Z., Teerlink, T., Griendling, K., Aslam, S., Welch, W.J., Wilcox, C.S., 2010. Angiotensin II and NADPH Oxidase Increase ADMA in Vascular Smooth Muscle Cells. Hypertension 56, 498–504. https://doi.org/10.1161/HYPERTENSIONAHA.110.152959

Mayer, S.A., Lignelli, A., Fink, M.E., Kessler, D.B., Thomas, C.E., Swarup, R., Van Heertum, R.L., 1998. Perilesional Blood Flow and Edema Formation in Acute Intracerebral Hemorrhage: A SPECT Study. Stroke 29, 1791–1798. https://doi.org/10.1161/01.STR.29.9.1791

Menon, R.S., Burgess, R.E., Wing, J.J., Gibbons, M.C., Shara, N.M., Fernandez, S., Jayam-Trouth, A., German, L., Sobotka, I., Edwards, D., Kidwell, C.S., 2012. Predictors of highly prevalent brain ischemia in intracerebral hemorrhage. Ann. Neurol. 71, 199–205. https://doi.org/10.1002/ana.22668

Morotti, A., Busto, G., Bernardoni, A., Marini, S., Casetta, I., Fainardi, E., 2020. Association Between Perihematomal Perfusion and Intracerebral Hemorrhage Outcome. Neurocrit. Care 33, 525–532. https://doi.org/10.1007/s12028-020-00929-z

Morotti, A., Busto, G., Boulouis, G., Scola, E., Bernardoni, A., Fiorenza, A., Amadori, T., Carbone, F., Casetta, I., Montecucco, F., Fainardi, E., 2022. Delayed perihematomal hypoperfusion is associated with poor outcome in intracerebral haemorrhage. Eur. J. Clin. Invest. 52, e13696. https://doi.org/10.1111/eci.13696

Periayah, M.H., Halim, A.S., Mat Saad, A.Z., 2017. Mechanism Action of Platelets and Crucial Blood Coagulation Pathways in Hemostasis. Int. J. Hematol.-Oncol. Stem Cell Res. 11, 319–327.

Prabhakaran, S., Naidech, A.M., 2012. Ischemic Brain Injury After Intracerebral Hemorrhage: A Critical Review. Stroke 43, 2258–2263. https://doi.org/10.1161/STROKEAHA.112.655910

Radomski, M.W., Palmer, R.M.J., Moncada, S., 1987. The anti-aggregating properties of vascular endothelium: interactions between prostacyclin and nitric oxide. Br. J. Pharmacol. 92, 639–646. https://doi.org/10.1111/j.1476-5381.1987.tb11367.x

Sapira, V., Cojocaru, I.M., Lilios, G., Grigorian, M., Cojocaru, M., 2010. Study of endothelin-1 in acute ischemic stroke. Romanian J. Intern. Med. Rev. Roum. Med. Interne 48, 329–332.

Schellinger, P.D., Fiebach, J.B., Hoffmann, K., Becker, K., Orakcioglu, B., Kollmar, R., Jüttler, E., Schramm, P., Schwab, S., Sartor, K., Hacke, W., 2003. Stroke MRI in Intracerebral Hemorrhage: Is There a Perihemorrhagic Penumbra? Stroke 34, 1674–1679. https://doi.org/10.1161/01.STR.0000076010.10696.55

Selim, M., Norton, C., 2020. Perihematomal edema: Implications for intracerebral hemorrhage research and therapeutic advances. J. Neurosci. Res. 98, 212–218. https://doi.org/10.1002/jnr.24372

Shah, R., 2007. Endothelins in health and disease. Eur. J. Intern. Med. 18, 272–282. https://doi.org/10.1016/j.ejim.2007.04.002

Shao, L., Chen, S., Ma, L., 2022. Secondary Brain Injury by Oxidative Stress After Cerebral Hemorrhage: Recent Advances. Front. Cell. Neurosci. 16, 853589. https://doi.org/10.3389/fncel.2022.853589

Valkonen, V.-P., Laakso, J., Päivä, H., Lehtimäki, T., Lakka, T.A., Isomustajärvi, M., Ruokonen, I., Salonen, J.T., Laaksonen, R., 2003. Asymmetrical dimethylarginine (ADMA) and risk of acute coronary events. Atheroscler. Suppl. 4, 19–22. https://doi.org/10.1016/S1567-5688(03)00029-1

Van Asch, C.J., Luitse, M.J., Rinkel, G.J., Van Der Tweel, I., Algra, A., Klijn, C.J., 2010. Incidence, case fatality, and functional outcome of intracerebral haemorrhage over time, according to age, sex, and ethnic origin: a systematic review and meta-analysis. Lancet Neurol. 9, 167–176. https://doi.org/10.1016/S1474-4422(09)70340-0

Wilkinson, D.A., Pandey, A.S., Thompson, B.G., Keep, R.F., Hua, Y., Xi, G., 2018. Injury mechanisms in acute intracerebral hemorrhage. Neuropharmacology 134, 240–248. https://doi.org/10.1016/j.neuropharm.2017.09.033

Won, S.J., Tang, X.N., Suh, S.W., Yenari, M.A., Swanson, R.A., 2011. Hyperglycemia promotes tissue plasminogen activator-induced hemorrhage by Increasing superoxide production. Ann. Neurol. 70, 583–590. https://doi.org/10.1002/ana.22538

Xie, J., Hong, E., Ding, B., Jiang, W., Zheng, S., Xie, Z., Tian, D., Chen, Y., 2020. Inhibition of NOX4/ROS Suppresses Neuronal and Blood-Brain Barrier Injury by Attenuating Oxidative Stress After Intracerebral Hemorrhage. Front. Cell. Neurosci. 14, 578060. https://doi.org/10.3389/fncel.2020.578060

Yanagisawa, M., Kurihara, H., Kimura, S., Tomobe, Y., Kobayashi, M., Mitsui, Y., Yazaki, Y., Goto, K., Masaki, T., 1988. A novel potent vasoconstrictor peptide produced by vascular endothelial cells. Nature 332, 411–415. https://doi.org/10.1038/332411a0

Yang, J., Jing, J., Chen, S., Liu, X., Tang, Y., Pan, C., Tang, Z., 2022. Changes in Cerebral Blood Flow and Diffusion-Weighted Imaging Lesions After Intracerebral Hemorrhage. Transl. Stroke Res. 13, 686–706. https://doi.org/10.1007/s12975-022-00998-6

Zahuranec, D.B., Lisabeth, L.D., Sánchez, B.N., Smith, M.A., Brown, D.L., Garcia, N.M., Skolarus, L.E., Meurer, W.J., Burke, J.F., Adelman, E.E., Morgenstern, L.B., 2014. Intracerebral hemorrhage mortality is not changing despite declining incidence. Neurology 82, 2180–2186. https://doi.org/10.1212/WNL.0000000000000519

Zhang, L., Li, Z., Feng, D., Shen, H., Tian, X., Li, H., Wang, Z., Chen, G., 2017. Involvement of Nox2 and Nox4 NADPH oxidases in early brain injury after subarachnoid hemorrhage. Free Radic. Res. 51, 316–328. https://doi.org/10.1080/10715762.2017.1311015

Ziv, I., Fleminger, G., Djaldetti, R., Achiron, A., Melamed, E., Sokolovsky, M., 1992. Increased plasma endothelin-1 in acute ischemic stroke. Stroke 23, 1014–1016. https://doi.org/10.1161/01.STR.23.7.1014

8. TABLES

Table 1. Clinical and demographic characteristics of patients according to presence/absence of ischemic lesions at T1.

	All patients	**Ischemic lesions**	**No ischemic lesions**	**p**
	N=28	**n=12**	**n=16**	
Demographic characteristics and clinical history				
Age, mean (SD)	70.2 (13.8)	68.4 (15.5)	70.8 (13.0)	0.661
Sex (female) (%)	13 (44.8)	6 (50)	6 (37.5)	0.508
Pre-stroke mRS (%)				
- 0	19/28 (67.9)	7/11 (63.6)	12 (75.0)	
- 1	5/28 (17.9)	2/11 (18.2)	3 (18.8)	
- 2	1/28 (3.6)	0	0	0.620
- 3	3/28 (10.7)	2/11 (18.2)	1 (6.3)	
- 4	0	0	0	
- 5	0	0	0	
Pre-stroke mRS 0-1 (%)	23/27 (85.2)	9/11 (81.8)	14/15 (93.3)	0.556
Smoking (%)				0.174
- no	7 (24.1)	3 (25.0)	4 (25.0)	

- current	15 (51.7)	8 (66.7)	6 (37.5)	
- previous	7 (24.1)	1 (8.3)	6 (37.5)	
Obesity (%)	7 (24.1)	3 (25.0)	4 (25.0)	1.0
Alcohol consumption (%)	2 (6.9)	0	2 (12.5)	0.492
Abuse drug consumption (%)	1 (3.4)	0	1 (6.3)	1.0
Hypertension (%)	22 (75.9)	12 (100.0)	9 (56.3)	**0.010**
Dyslipidemia (%)	10 (34.5)	9 (75.0)	1 (6.3)	**<0.001**
Atrial fibrillation (%)	6 (20.7)	2 (16.7)	3 (18.8)	1.0
Ischemic cardiopathy (%)	4 (13.8)	1 (8.3)	3 (18.8)	0.613
Diabetes Mellitus (%)	7 (24.1)	4 (33.3)	3 (18.8)	0.418
Previous stroke (%)	2 (6.9)	0	2 (12.5)	0.492
Previous TIA (%)	0	0	0	-
Coagulopathy (%)	1 (3.4)	0	1 (6.3)	1.0
Valvulopathy (%)	2 (6.9)	0	1 (6.3)	1.0
Peripheral vasculopathy (%)	1 (3.4)	0	1 (6.3)	1.0
Migraine (%)	0	0	0	-
Cancer (%)	2 (6.9)	1 (8.3)	1 (6.3)	1.0
Stressful events (%)	3 (10.3)	1 (8.3)	2 (12.5)	1.0

Therapy before hemorrhagic stroke				
Anticoagulants (%)	7 (24.1)	2 (16.7)	4 (25.0)	0.673
Antiplatelets (%)	8 (28.6)	4/11 (36.4)	4 (25.0)	0.675
Lipid lowering medications (%)	2 (6.9)	2 (16.7)	0	0.175
ACE-1/ARB (%)	12 (42.9)	7/11 (63.6)	4 (25.0)	0.061
Diuretics (%)	5 (17.2)	2 (16.7)	2 (12.5)	1.0
Beta-blockers (%)	5 (17.2)	3 (25.0)	2 (12.5)	0.624
Alpha-lytics (%)	4 (13.8)	3 (25.0)	1 (6.3)	0.285
Calcium-antagonists (%)	0	0	0	-
PPI (%)	3 (10.3)	1 (8.3)	2 (12.5)	1.0
Blood glucose lowering medications (%)	3 (10.3)	2 (16.7)	1 (6.3)	0.560
Insulin (%)	0	0	0	-
Nitrates (%)	0	0	0	-
Clinical characteristics of hemorrhagic stroke				
Stroke on awakening (%)	11/29 (37.9)	7 (58.4)	4 (25.0)	0.121
NIHSS, median (IQR)				
- Admission (T0)	11 (7.5-18)	14 (6.75-17.50	9 (7.25-18.25)	0.642

- 12-24 h (T1)	9 (6.5-13.5)	13 (6-20)	9 (7.75-10.50)	0.667
- 48-72 h (T2)	10 (7.5-14.5)	14 (6-20)	8.50 (7.75-10.50)	0.197
- Discharge	7 (5-11.5)	8 (4-12.50)	6 (5-11)	0.720
SBP, mean (SD)				
- T0	168.4 (31.50)	168.5 (30.3)	168.9 (34.4)	0.977
- T1	145.8 (25.9)	150.1 (24.3)	140.7 (29.0)	0.534
- T2	147.2 (22.4)	149.9 (13.9)	143.4 (32.7)	0.646
DBP, mean (SD)				
- T0	92.57 (19.21)	91.4 (20.1)	94.0 (19.7)	0.740
- T1	85.8 (17.6)	88.9 (16.1)	81 (19.4)	0.387
- T2	84.1 (16.7)	83.3 (10.0)	85.2 (24.8)	0.855
HR, mean (SD)				
- T0	80.6 (13.71)	78.6 (15.5)	81.1 (12.6)	0.652
- T1	81.2 (21.2)	88 (22.6)	73.3 (18.1)	0.228
- T2	79.3 (12.3)	83.9 (19.6)	73.0 (10.0)	0.362
Body temperature, mean (SD)				
- T0	36.0 (0)	36 (0)	36.0 (0)	-
- T1	36.9 (0.70)	27.2 (0.8)	36.6 (0.3)	0.108
- T2	36.9 (0.6)	37.2 (0.4)	36.6 (0.6)	**0.043**

HGT, mean (SD)				
- T0	128 (29.4)	136 (32.9)	120 (24.6)	0.143
- T1	128 (32.7)	128 (30.9)	130 (38.7)	0.949
- T2	119 (23.0)	118 (25.8)	120 (97.5-137.5)	0.900
Craniotomy (%)	3/19 (15.8)	2/8 (25.0)	1/11 (9.1)	0.546

Scheme 1. SD= standard deviation; ACE-1/ARBs= angiotensin converting enzyme inhibitors/angiotensin II receptor blockers; PPIs= Proton-Pump Inhibitors; NIHSS= National Institutes of health Stroke Scale; IQR= Interquartile range**;** SBP= systolic blood pressure; DBP= diastolic blood pressure; HR= heart rate; HGT= Hemo Glucose Test.

Table 2. Blood test results of patients according to presence/absence of ischemic lesions at T1.

	All patients **N=28**	**Ischemic lesions** **n=12**	**No ischemic lesions** **n=16**	**p**
Routine blood tests				
Time onset-blood sampling T0, h, median (IQR)	2.08 (1.27-2.57)	2.33 (1.24-4.19)	2.07 (1.14-2.41)	0.429
Time onset-T1, h, median (IQR)	26.50 (25.30-27.30)	26.5 (25.6-29.5)	26.60 (25.10, 27.58)	0.927
Time onset-T2, h median (IQR)	51.0 (48.5-53.2)	51 (50.25-54.60)	49.9 (48.3-52.9)	0.361
Haematocrit, T0, mean (SD)	40.5 (5.1)	38.7 (5.2)	42.2 (4.7)	0.073
Platelets, T0, mean (SD)	232.5 (74.95)	233.3 (67.3)	222.8 (75.2)	0.703
Total leukocytes, mean (SD)				
- T0	8.66 (2.96)	10.18 (3.31)	7.42 (2.17)	**0.013**
- T1	10.51 (5.24)	12.32 (5.90)	7.50 (2.21)	0.234
- T2	11.83 (7.87)	13.52 (9.40)	8.46 (1.32)	0.400
Neutrophils (absolute number), mean (SD)				
- T0	6.13 (2.91)	7.44 (3.26)	4.49 (2.35)	**0.037**

- T1	8.46 (5.11)	10.2 (5.83)	5.64 (2.06)	0.254
- T2	9.94 (7.36)	11.55 (8.76)	6.71 (1.14)	0.387
Neutrophils (%)				
- T0	68.90 (12.94)	71.20 (11.88)	67.4 (14.2)	0.456
- T1	77.56 (8.06)	79.62 (9.25)	74.13 (5.26)	0.392
- T2	81.86 (5.26)	83.23 (6.03)	79.10 (1.66)	0.295
Lymphocytes (absolute number), mean (SD)				
- T0	1.84 (1.03)	1.94 (1.0)	1.70 (1.08)	0.555
- T1	77.56 (8.06)	1.31 (0.62)	1.11 (0.19)	0.612
- T2	1.08 (0.35)	1.09 (0.43)	1.06 (0.16)	0.912
Lymphocytes (%), mean (SD)				
- T0	22.40 (11.35)	20.24 (9.71)	23.69 (12.81)	0.443
- T1	13.60 (5.95)	12.68 (7.52)	15.13 (2.29)	0.612
- T2	10.41 (3.20)	9.23 (3.36)	12.77 (0.56)	0.123
PCR (mg/dL), mean (SD)				
- T0	0.51 (0.72)	0.79 (0.97)	0.23 (0.24)	0.111
- T1	2.33 (1.68)	3.10 (1.59)	1.06 (0.95)	0.094
- T2	6.17 (6.19)	8.70 (6.75)	1.94 (0.07)	0.144

INR, T0, mean (SD)	1.09 (0.22)	1.04 (0.10)	1.13 (0.28)	0.253
PTT ratio, T0, mean (SD)	0.96 (0.23)	0.94 (1.76)	0.97 (0.27)	0.804
Fibrinogen (md/dL), T0, mean (SD)	374.38 (90.50)	389.3 (84.5)	358.81 (96.37)	0.391
Total cholesterol (mg/dL), T0, mean (SD)	162.63 (32.02)	161.0 (21.6)	164.3 (43.8)	0.898
LDL (md/dL), T0, mean (SD)	103.25 (23.40)	109.5 (19.7)	97.0 (28.0)	0.493

Scheme 2. IQR= Interquartile range; SD=standard deviation; PCR= Polymerase Chain Reaction; INR= International Normalized Ratio; PTT= Prothrombin Time Test; LDL= Low Density Lipoproteins.

9. FIGURES

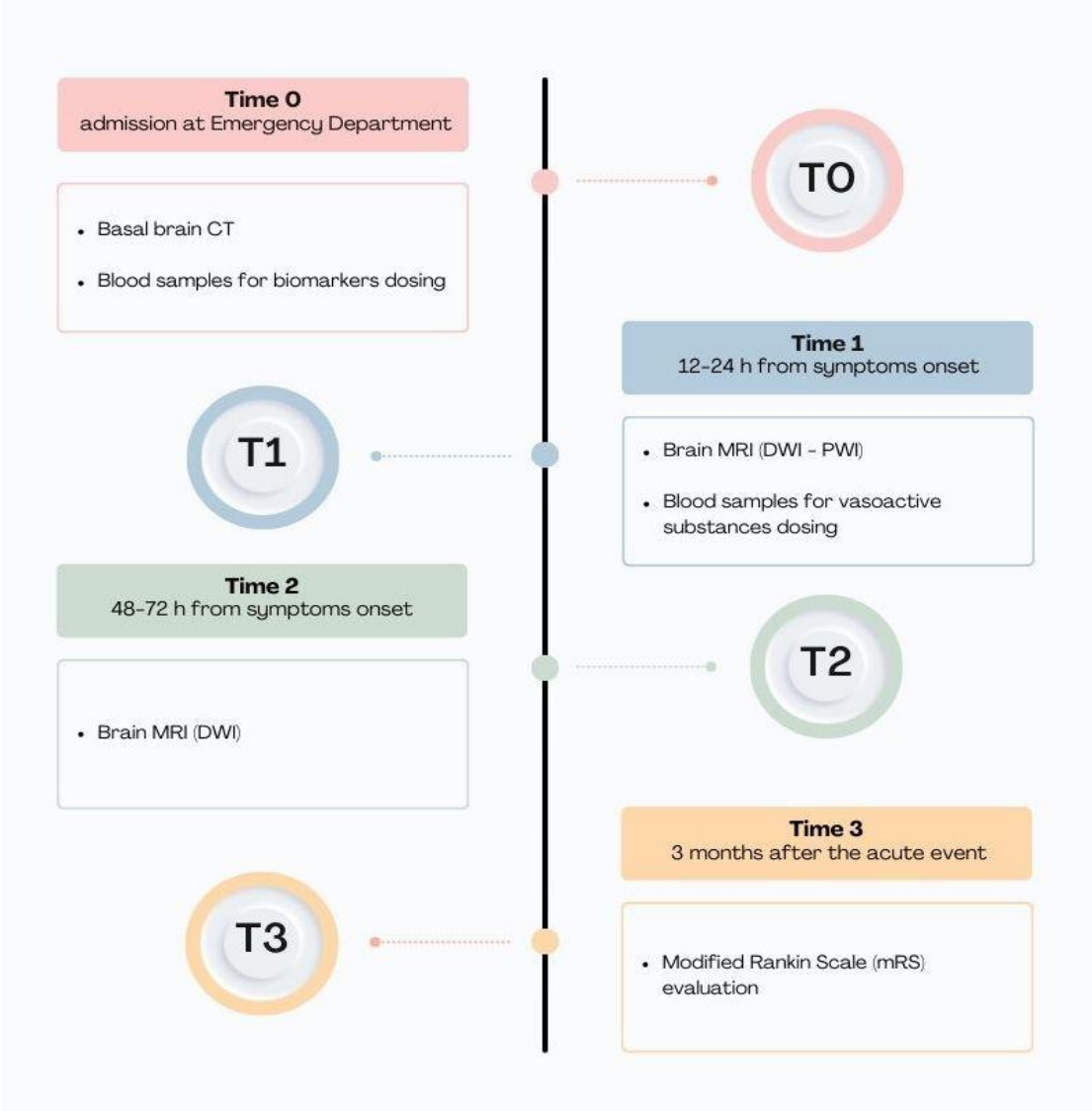

Figure 1. Study timeline.

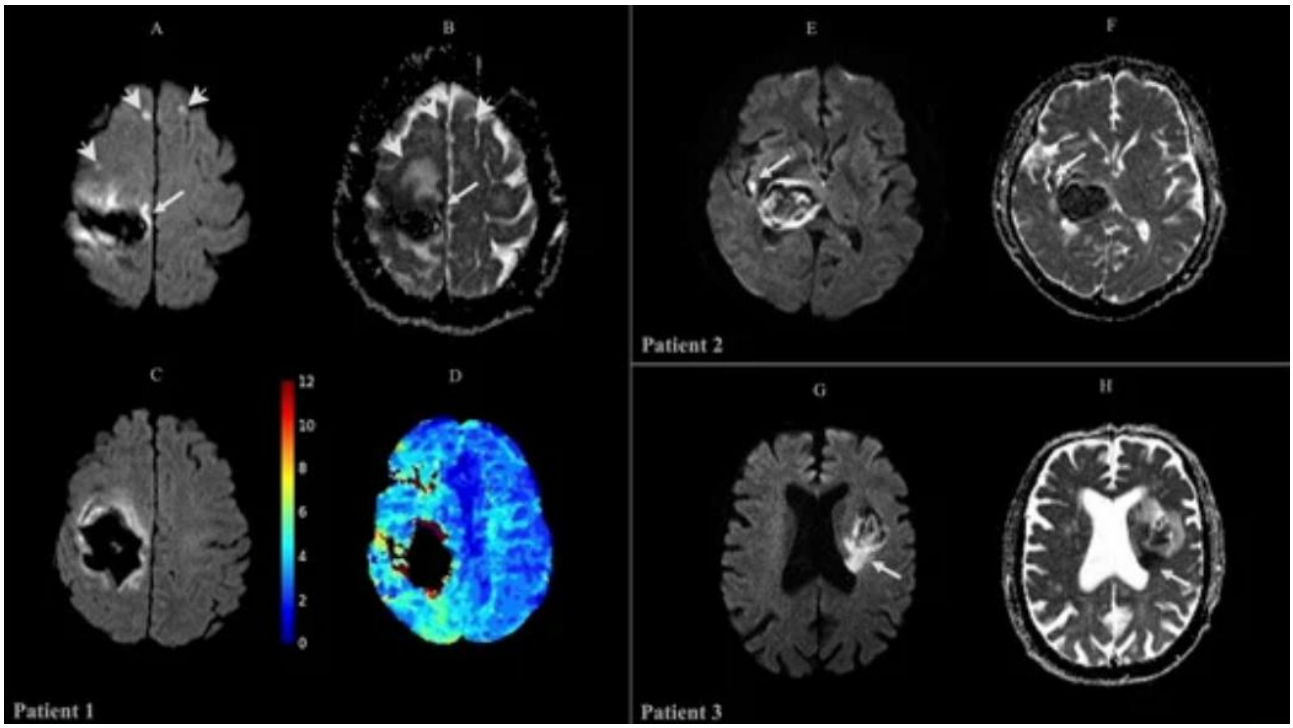

Figure 2. Representative neuroimaging of three patients.

Patient 1. MRI imaging at T2 reveals a large intraparenchymal hematoma within the right fronto-parietal lobe. (**A**) DWI sequences identify linear regions of restricted diffusion in the anterior perilesional area and the posteromedial region, with corresponding hypointensity on ADC map (**B**), suggestive of ischemic injury (**arrow**). Additionally, small ischemic foci, measuring a few millimeters, are observed in the right frontal subcortical paramedian region and at the left frontal subcortical level (**arrowheads**). (**D**) Perfusion-weighted imaging (PWI) shows a significant increase of Tmax within the right parieto-occipital region and posterior temporal lobe, surrounding a large hematoma located in the right fronto-parietal lobe (**C**).

Patient 2. MRI imaging at T1 demonstrates a hematoma located in the right thalamo-capsular region with slight contralateral shift of the midline structures. (**E**) DWI imaging shows a perihematomal 5 mm^2 area of diffusion restriction, with corresponding hypointensity on the ADC map (**F**), consistent with a small recent ischemic lesion (**arrow**).

Patient 3. MRI imaging at T1 reveals a hemorrhagic focus in the left insula and basal ganglia, with slight lateral ventricle compression. (**G**) DWI imaging demonstrates a region of restricted diffusion

in the posteromedial perilesional area, with corresponding hypointensity on ADC map (**H**), suggestive of ischemic injury (**arrow**).

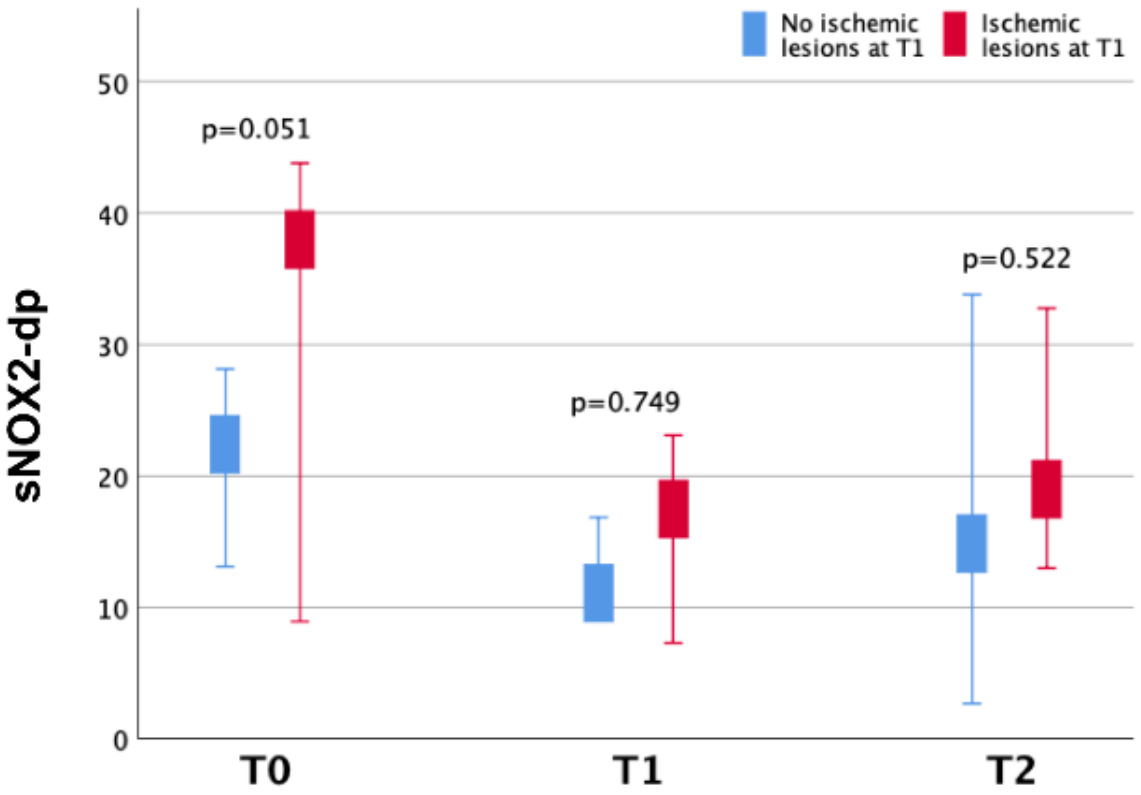

Figure 3. Median plasma levels (pg/mL) of sNOX2-dp at different timepoints (T0, T1, T2) by presence/absence of ischemic lesions at T1.

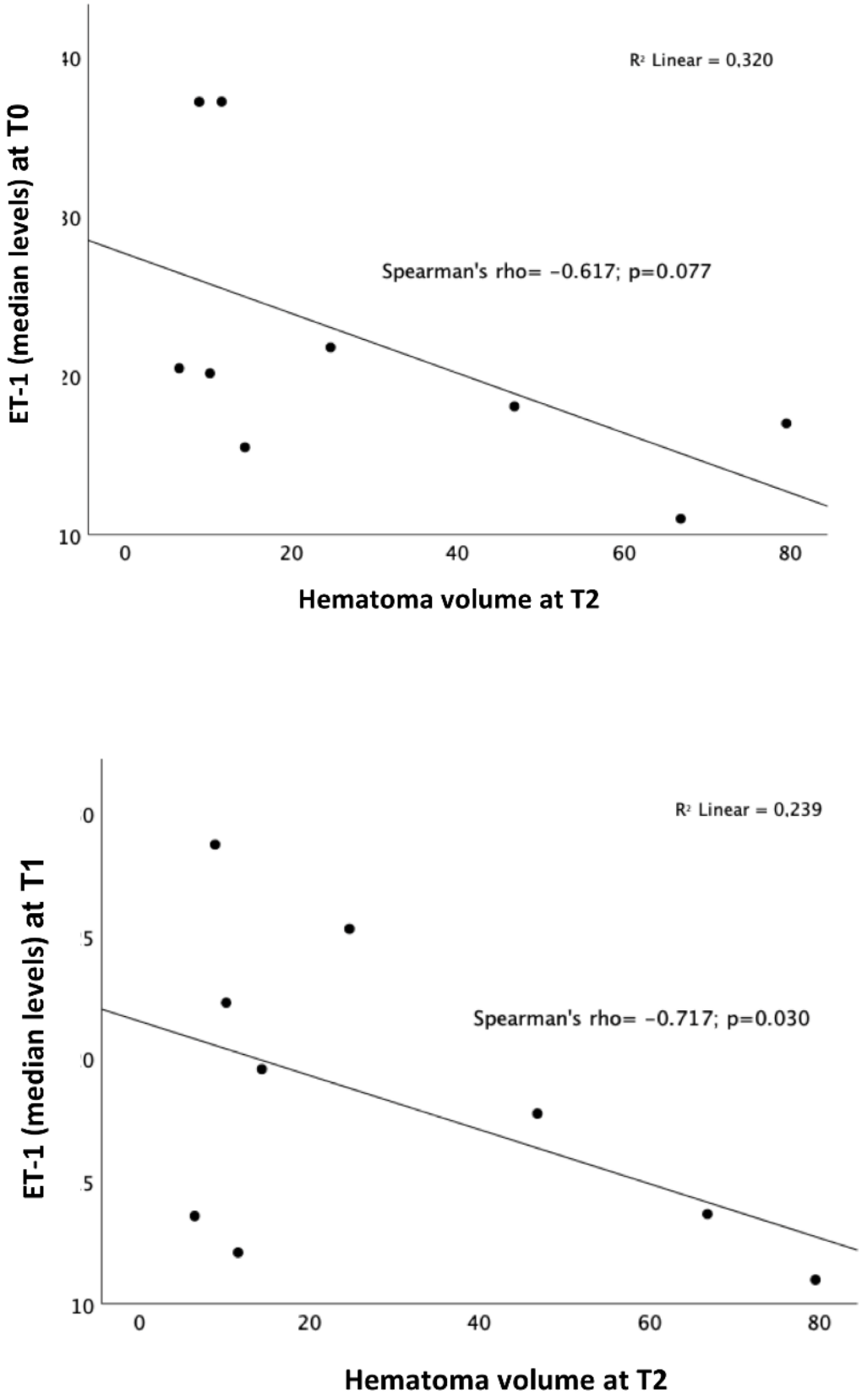

Figure 4. Correlations between ET-1 levels at T0 and T1 and hematoma volume at T2.

The statistical test is the Spermann correlation test; black dots represent the single data points; ET-1 levels were measured in pg/mL; hematoma volume was measured in cm^3.

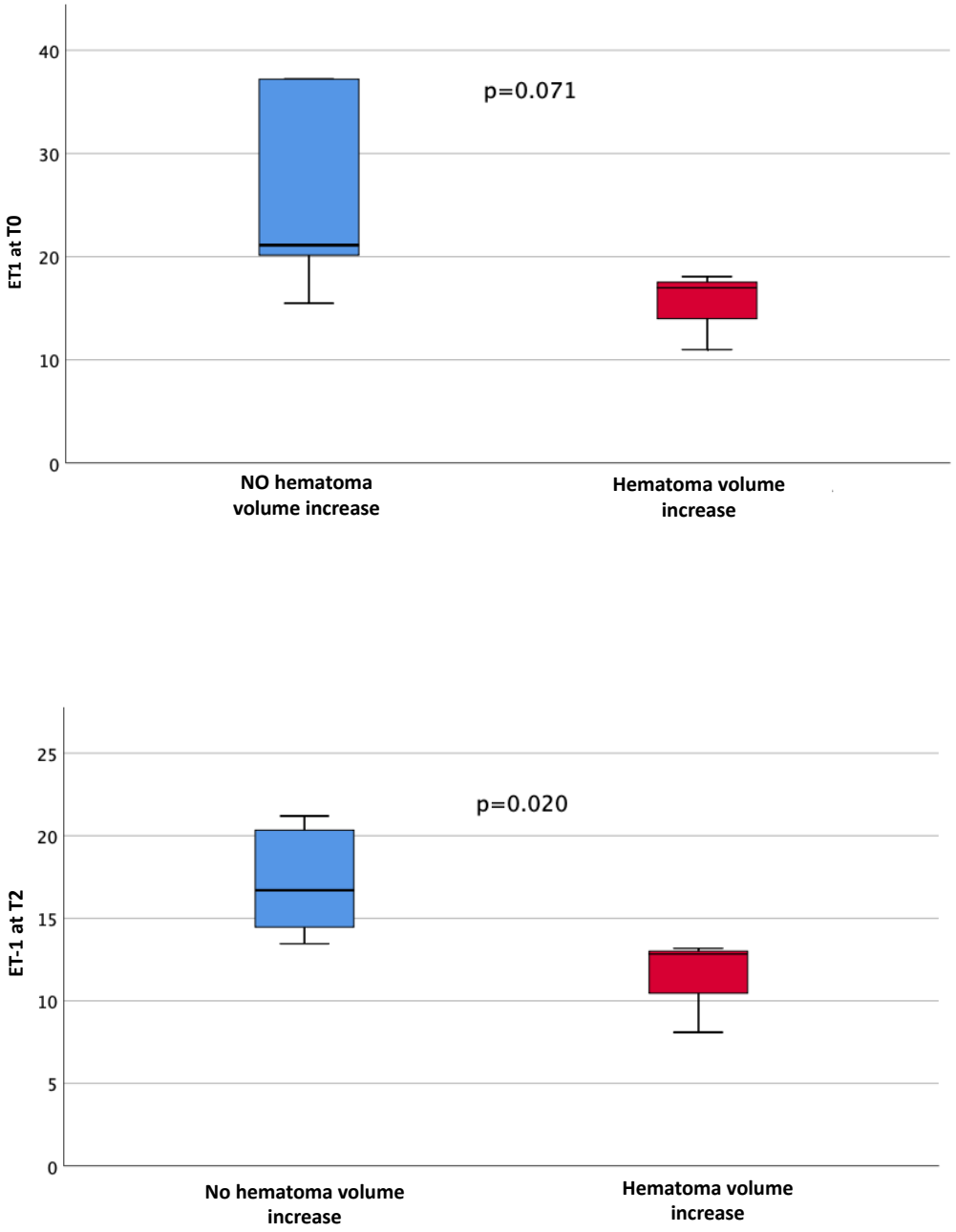

Figure 5 Associations between ET-1 levels (pg/mL) at T0 and T2 and hematoma volume increase from T1 to T2.

10. SUPPLEMENTARY MATERIALS

Supplementary Table 1. Radiological characteristics of hemorrhagic stroke in all study patients and by presence/absence of ischemic lesions at T1 (statistically significant differences are in bold)

	All patients N=28	**Ischemic lesions n=12**	**No ischemic lesions n=16**	**p value**
Angiography (%)				0.493
- no	14/18 (77.8)	8/10 (80.0)	6/8 (75.0)	
- yes	3/18 (16.7)	2/10 (20.0)	1/8 (12.5)	
- yes, pathologic	1/18 (5.6)	0	1/8 (12.5)	
Hematoma side (%)				0.304
- left	14/28 (50.0)	4 (33.3)	10 (62.5)	
- right	12/28 (42.9)	7 (58.3)	5 (31.3)	
- bilateral	2/28 (7.1)	1 (8.3)	1 (6.3)	
Hematoma localization (%)				0.704
- deep	13/27 (48.1)	5 (41.7)	8/15 (53.3)	
- lobar	14/27 (51.9)	7 (58.3)	7/15 (46.7)	
T1				
Time of onset-CT at T1, h, median (IQR)	2.3 (1.5-3.2)	2.0 (1.4-5.7)	2.32 (1.47-3.50)	0.875
Time of onset-MRI at T1, h, median (IQR)	9.9 (3.3-21.8)	14.8 (4.8-20.3)	6.95 (3.23-22.70)	0.947
Hematoma volume at T1, median (IQR), cm3	11.9 (5.8-32.1)	23.05 (13.40-41.03)	6.65 (2.85-12.40)	**0.005**
Peri-hematoma edema at T1 (%)				0.131
- absent	2/28 (7.1)	0	2 (12.5)	
- cortical sulci narrowing	3/28 (10.7)	0	3 (18.8)	
- ventricles asymmetry	10/28 (35.7)	4 (33.3)	6 (37.5)	
- midline shift	13/28. (46.4)	8 (66.7)	5 (31.3)	
Edema severity at T1 (%)				0.063
- Absent/mild/moderate	15/28 (53.6)	4 (33.3)	11 (68.8)	
- Severe	13/28 (46.4)	8 (66.7)	5 (31.3)	
Peri-hematoma edema volume at T1, median (IQR), cm3	11.40 (4.13-19.33)	15.25 (11.05-27.78)	8.15 (3.85-12.20)	**0.046**
Midline shift at T1, mm, mean (SD)	2.59 (3.89)	4.45 (4.74)	1.31 (2.62)	**0.036**
Intraventricular hemorrhage at T1 (%)	14/28 (50.0)	8 (66.7)	6 (37.5)	0.127
Ischemic lesions at T1 (%)	12/28 (42.9)		-	-
- Not remote	11/28 (39.3)	11 (91.7)		
- Remote	1/28 (3.6)	1 (8.3)		

Number of ischemic lesions a T1 (%)	12/28 (42.9)	12 (100.0)	-	-
- single	7/28 (25.0)	7 (58.3)		
- multiple	5/28 (17.9)	5 (41.7)		
Remote ischemic lesions at T1 (%)	1/28 (3.6)	1 (8.3)	-	-
- ipsilateral	0	0		
- controlateral	1/28 (3.6)	1 (8.3)		
Ischemic lesions morphology at T1 (%)			-	-
- perihematomal	6/12 (50.0)	6/12 (50.0)		
- not perihematomal	6/12 (50.0)	6/12 (50.0)		
Island sign at T1 (%)	14/27 (51.9)	10 (83.3)	4/15 (26.7)	**0.003**
Hemispheric hypoperfusion at T1 (%)	5/26 (19.2)	4/10 (40.0)	1 (6.3)	0.055
Fazekas Scale (%)				0.464
- 0 (absent/very mild)	3 (11.1)	1/11 (9.1)	2 (12.5)	
- 1 (mild)	10 (37.0)	4/11 (36.4)	6 (37.5)	
- 2 (moderate)	8 (29.6)	2/11 (18.2)	6 (37.5)	
- 3 (severe)	6 (22.2)	4/11 (36.4)	2 (12.5)	
Fazekas Scale (%)				0.816
- 0-1 (absent-mild)	13/27 (48.1)	5/11 (45.5)	8 (50.0)	
- 2-3 (moderate-severe)	14/27 (51.9)	6/11 (54.5)	8 (50.0)	
Microbleeds (%)				0.432
- absent	19/28 (67.9)	7 (58.3)	12 (75.0)	
- present	9/28 (32.1)	5 (41.7)	4 (25.0)	
Number of microbleeds (%)				
- ≤10	7/9 (77.8)	4 (33.3)	3 (18.8)	0.387
- >10	2/28 (22.8)	1 (8.3)	1 (6.3)	0.835
T2				
Time of onset-MRI at T2, h, median (IQR)	67.1 (53.5-110.3)	59.2 (47.0-110.9)	75.71 (53.60-110.29)	0.753
Hematoma volume at T2, mean (IQR), cm3	10.20 (6.8-36.5)	19.55 (9.80-42.05)	6.90 (6.20-27.70)	**0.043**
Hemorrhage volume variation from T1 to T2, mean (IQR), cm3	-1.1 (-2.30, 3.25)	-0.65 (-4.45, 2.28)	-1.10 (-1.80, 3.70)	0.531
Hematoma volume increase (%)	5/17 (29.4)	2/8 (25.0)	3/9 (33.3)	1.0
Perihematomal edema at T2 (%)				**0.040**
- absent	2/18 (11.1)	0	2/10 (20.0)	-
- cerebral sulci	1/18 (5.6)	0	1/10 (10.0)	-
- ventricles asymmetry	6/18 (33.3)	1/8 (12.5)	5/10 (50.0)	0.103
- midline shift	9/18 (50.0)	7/8 (87.5)	2/10 (20.0)	**0.006**
Edema severity at T2 (%)				**0.015**
- Absent/mild/severe	9/18 (50.0)	1/8 (12.5)	8/10 (80.0)	
- Severe	9/18 (50.0)	7/8 (87.5)	2/10 (20.0)	

Perihematomal edema volume at T2, mean (IQR), cm3	23.50 (13.7-38.5)	38.0 (20.18-43.08)	14.80 (9.85-23.65)	**0.012**
Edema volume variation from T1 to T2, median (IQR), cm3	4.8 (1.2, 15.4)	12.50 (-2.03, 19.0)	4.3 (3.10, 13.20)	0.596
Edema volume increase (%)	13/16 (81.3%)	5/7 (71.4)	8/9 (88.9)	0.550
Midline shift at T2, mm, mean (SD)	2.94 (3.54)	4.75 (3.22)	1.3 (2.99)	**0.035**
Intraventricular hemorrhage at T2 (%)	6/17 (35.3)	3/7 (42.9)	3/10 (30.0)	0.644
Ischemic lesions at T2 (%)	9/15 (60.0)	6/7 (85.7)	3/8 (37.5)	0.066
- Not remote	7/15 (46.7)	4/7 (57.1)	3/8 (37.5)	0.462
- Remote	2/15	2/7 (28.6)	0	0.200
Number of ischemic lesions at T2 (%)	9/15 (60.0)	6/7 (85.6)	3/8 (37.5)	0.066
- single	3/15 (20.0)	2/7 (28.6)	1/8 (12.5)	0.453
- multiple	6/15 (40.0)	4/7 (57.1)	2/8 (25.0)	0.220
Remote ischemic lesions at T2 (%)	2/15 (13.3)	2/7 (28.6)	0	0.200
- ipsilateral	2/15 (13.3)	2/7 (28.6)		
- controlateral	0	0		
New ischemic lesions at T2 vs at T1 (%)	3/16 (18.8)	0	3/8 (37.5)	0.200
Ischemic lesions at T1 not visible at T2 (%)	2/16 (12.5)	2/8 (25.0)	0	0.467

IQR= interquartile range; SD= standard deviation.

Supplementary Table 2. Clinical outcome measures in all study patients and by presence/absence of ischemic lesions at T1

	All patients N=28	**Ischemic lesions n=12**	**No ischemic lesions n=16**	**p value**
mRS at 3 months (%)				0.082
- 0	2/23 (8.7)	2/8 (25.0)	0	
- 1	2/23 (8.7)	0	2/14 (14.3)	
- 2	4/23 (17.4)	0	4/14 (28.6)	
- 3	2/23 (8.7)	1/8 (12.5)	1/14 (7.1)	
- 4	2/23 (8.7)	2/8 (25.0)	0	
- 5	1/23 (4.3)	0	1/14 (7.1)	
- 6	10/23 (43.5)	3/8 (37.5)	6/14 (42.9)	
mRS at 3 months 0-1 (%)	4/23 (17.4)	2/8 (25.0)	2/14 (14.3)	0.602
mRS at 3 months 0-2 (%)	8/23 (34.8)	2/8 (25.0)	6/14 (42.9)	0.649
mRS at 3 months 0-3 (%)	10/23 (43.5)	3/8 (37.5)	7/14 (50.0)	0.675
mRS at 3 months 2-6 (%)	19/23 (82.6)	6/8 (75.0)	12/14 (85.7)	0.602

mRS at 3 months 3-6 (%)	15/23 (65.2)	6/8 (75.0)	8/14 (57.1)	0.649
mRS at 3 months 4-6 (%)	13/23 (56.5)	5/8 (62.5)	7/14 (50.0)	0.675
Intrahospital death (%)	10 (34.5)	3 (25.0)	6 (37.5)	0.687
Death at 3 months (%)	10/23 (43.5)	3/8 (37.5)	6/14 (42.9)	1.0

mRS= modified Rankin Scale

Supplementary Table 3. Plasma levels of molecular biomarkers at various timepoints (T0, T1, T2) in all study patients and by presence/absence of ischemic lesions at T1 (statistically significant or borderline statistically significant differences are in bold)

	All patients N=28	**Ischemic lesions n=12**	**No ischemic lesions n=16**	**p value**
NO, μM, mean (IQR)				
- T0	18.42 (8.68-28.62)	15.02 (6.35-27.40)	19.71 (9.0-30.58)	0.386
- T1	22.76 (19.04-42.66)	20.69 (18.45-39.0)	29.40 (17.03-44.69)	0.749
- T2	28.39 (15.35-48.34)	28.52 (14.89-48.34)	28.08 (16.44-65.53)	1.0
ET-1, pg/mL, mean (IQR)				
- T0	18.74 (14.05-22.12)	19.92 (17.19-33.43)	16.40 (11.38-20.22)	0.110
- T1	15.71 (12.46-21.62)	18.67 (11.81-26.15)	13.66 (13.02-20.29)	0.630
- T2	13.96 (12.15-17.63)	15.07 (11.91-17.63)	13.65 (10.78-19.51)	0.831
sNOX2-dp, pg/mL mean (IQR)				
- T0	27.51 (18.91-37.30)	34.94 (27.96-42.0)	22.40 (18.37-27.75)	**0.051**
- T1	14.50 (9.41-19.79)	17.50 (8.59-20.92)	11.57 (9.52-17.87)	0.749
- T2	18.73 (12.07-24.20)	18.99 (14.50-24.20)	14.84 (4.34-20.43)	0.522
ADMA, ng/mL, mean (IQR)				
- T0	128.70 (111.73-169.43)	167.94 (119.43-175.07)	121.89 (103.67-146.92)	0.131
- T1	110.69 (98.78-120.33)	99.44 (94.28-116.27)	116.55 (106.67-146.20)	0.078
- T2	116.56 (92.06-126.77)	116.56 (97.20-126.34)	107.56 (91.97-144.70)	0.831

NO= nitric oxide; IQR= Interquartile range; ET-1= endothelin 1; sNOX2-dp = soluble NOX2-derived peptide; ADMA= asymmetric dimethyl-arginine.

Supplementary Table 4. Median changes in plasma levels of molecular biomarkers over time in all study patients and by presence/absence of ischemic lesions at T1 (statistically significant differences are in bold)

	All patients N=28	**Ischemic lesions n=12**	**No ischemic lesions n=16**	**p value**
NO, μM, mean (IQR)				
- ΔT1-T0	9.97 (-8.86, 20.79)	9.54 (-1.88, 16.46)	20.79 (-9.11, 29.27)	0.361
- ΔT2-T1	5.96 (-14.33, 24.90)	9.23 (-11.21, 24.90)	-3.82 (-18.78, 24.82)	0.670
- ΔT2-T0	20.62 (-7.24, 29.88)	21.13 (-21.30, 0.78)	11.81 (-3.72, 46.63)	0.831
ET-1, pg/mL, mean (IQR)				
- ΔT1-T0	-0.23 (-6.66, 2.53)	-3.16 (-12.63, 3.66)	-1.09 (-5.59, 2.27)	0.631
- ΔT2-T1	-2.08 (-8.28, 1.58)	-3.93 (-10.26, 1.58)	-1.05 (-6.18, 5.50)	0.394
- ΔT2-T0	-2.62 (-12.60, 0.84)	-6.89 (-21.30, 0.78)	-0.34 (-4.61, 1.56)	0.136
sNOX2-dp, pg/mL, mean (IQR)				
- ΔT1-T0	-13.32 (-19.28, -4.60)	-18.56 (-23.78, -12.37)	-7.24 (-12.18, -2.31)	**0.037**
- ΔT2-T1	-1.83 (-3.82, 16.47)	-1.83 (-3.70, 16.47)	0.13 (-5.98, 19.21)	0.831
- ΔT2-T0	- 17.66 (-20.70, 0.22)	-18.77 (-23.12, -5.19)	-10.90 (-18.59, 14.56)	0.286
ADMA, ng/mL, mean (IQR)				
- ΔT1-T0	-30.72 (-45.20, -6.42)	-38.04 (-61.38, -21.45)	-16.27 (-34.24, 45.25)	0.150
- ΔT2-T1	-7.15 (-19.88, 31.84)	10.86 (-16.20, 31.84)	-18.46 (-25.52, 30.33)	0.394
- ΔT2-T0	-37.02 (-54.56, 10.39)	-49.86 (-58.58, 10.39)	-13.65 (-47.13, 22.44)	0.286

NO= nitric oxide; IQR= Interquartile range; ET-1= endothelin 1; sNOX2-dp = soluble NOX2-derived peptide; ADMA= asymmetric dimethyl-arginine.

Supplementary Figure 1. Median plasma levels of molecular biomarkers at different timepoints (T0, T1, T2) by presence/absence of ischemic lesions at T1.

A. NO (plasma levels in μM); B. ET-1 (plasma levels in pg/mL); C. ADMA (plasma levels in ng/mL)

A.

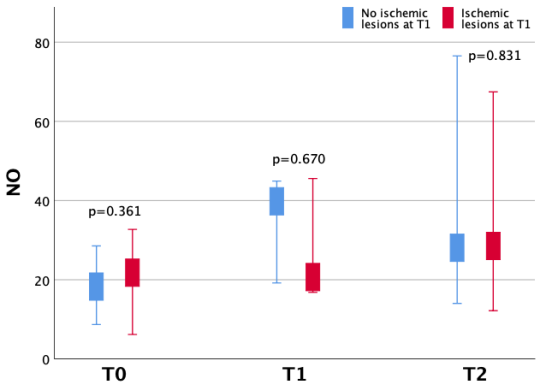

B.

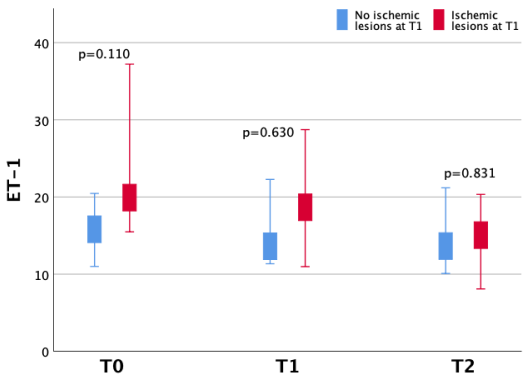

C.

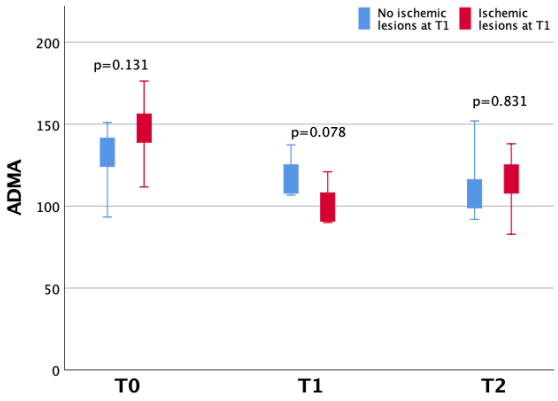

Supplementary Figure 2. Time profile of median plasma levels of molecular biomarkers at different timepoints by presence/absence of ischemic lesions at T1.

A. NO (plasma levels in μM); B. ET-1 (plasma levels in pg/mL); C. sNOX2-dp (plasma levels in pg/mL); D. ADMA (plasma levels in ng/mL)

A.

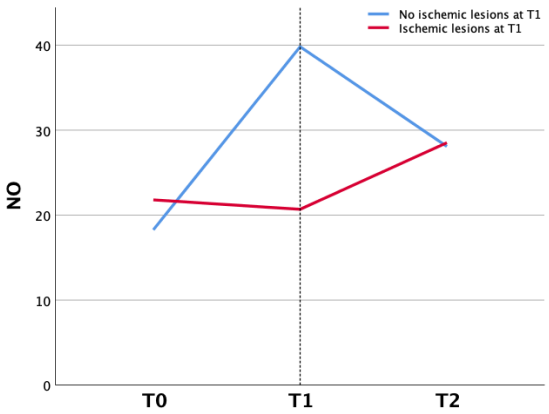

B.

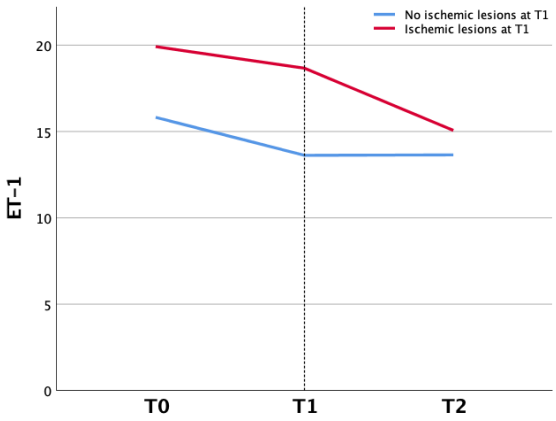

C.

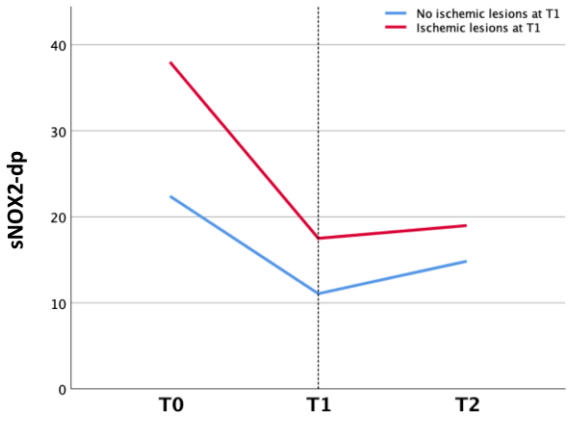

D.

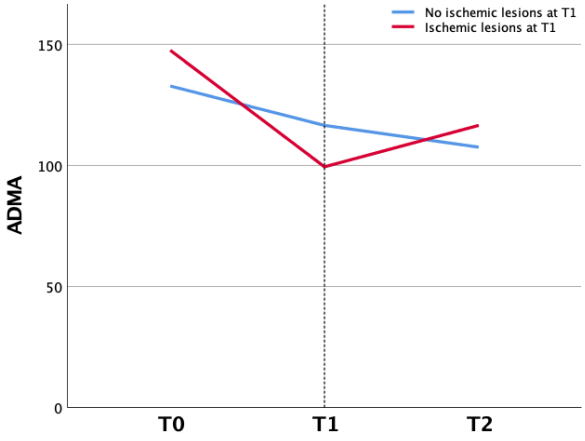

Supplementary Figure 3. Associations between molecular biomarkers and hemispheric hypoperfusion at T1.

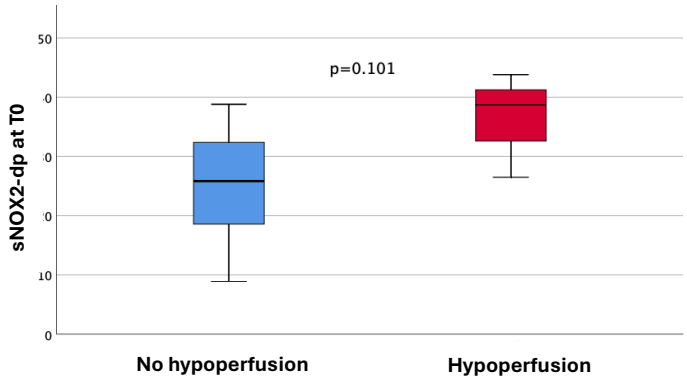

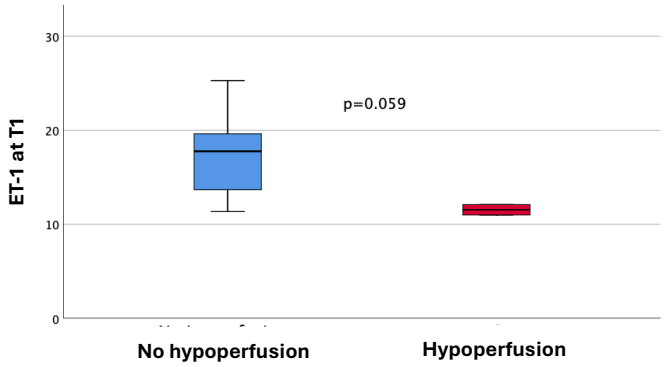

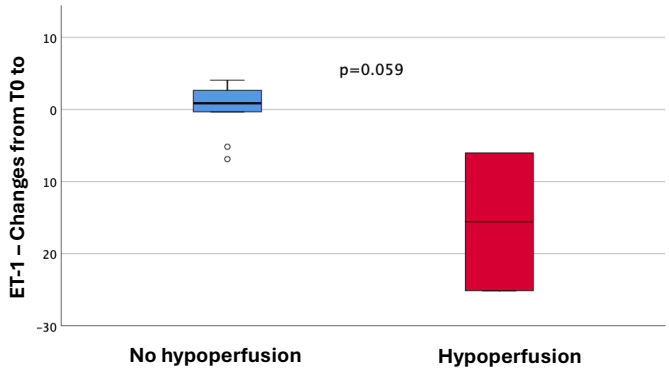

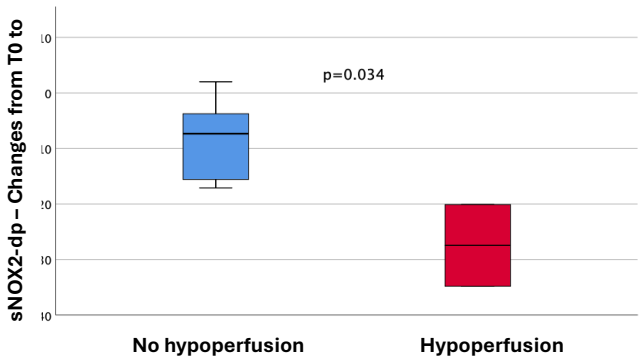

	No hypoperfusion (n=14)	Hypoperfusion (n=3)	p value
sNOX2-dp at T0, pg/mL, median (min, max)	25.85 (8.91, 38.80)	38.69 (26.49, 43.81)	0.101
ET-1 at T1, pg/mL, median (min, max)	17.76 (11.35, 25.29)	11.54 (10.98, 12.09)	0.059
ET-1 T0-T1, pg/mL, median (min, max)	0.88 (-6.88, 4.08)	-15.57 (-25.12, -6.01)	0.059
sNOX2-dp T0-T1, pg/mL, median (min, max)	-7.33 (-17.11, 2.0)	-27.45 (-34.79, -20.11)	0.034

Supplementary Figure 4. Associations between molecular biomarkers and severity of brain edema at T2

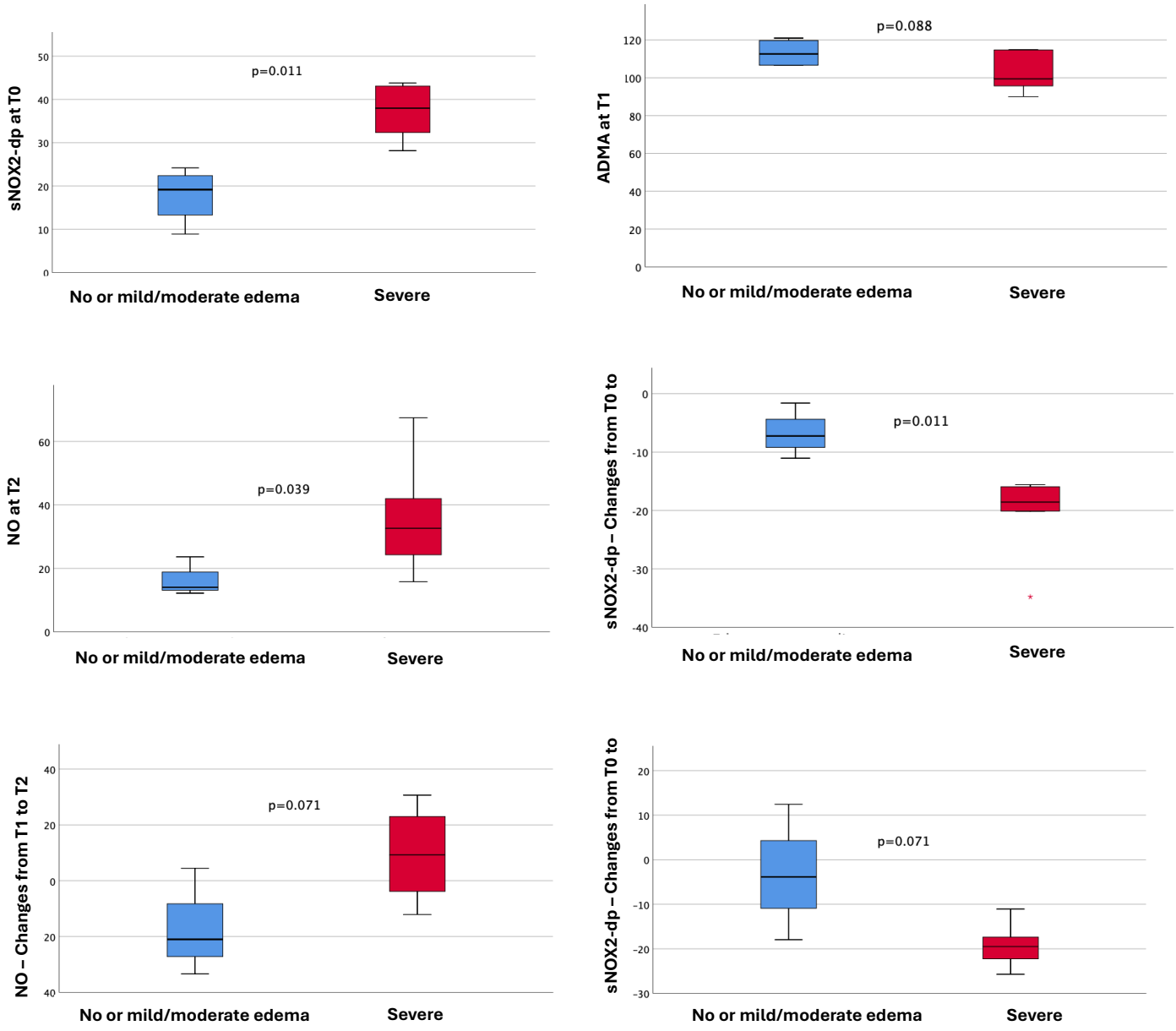

	No or mild-moderate edema (n=4)	Severe edema (n=6)	p value
sNOX2-dp at T0, pg/mL, median (min, max)	19.17 (11.11, 23.29)	37.99 (31.32, 43.28)	0.011
ADMA at T1, ng/mL, median (min, max)	112.57 (106.59, 120.33)	99.44 (94.28, 114.68)	0.088
NO at T2, μM, median (min, max)	14.03 (12.18, …)	32.64 (22.15, 48.34)	0.039
sNOX2-dp T0-T1, pg/mL, median (min, max)	-7.24 (-10.12, -2.99)	-18.56 (-23.78, -15.86)	0.011
NO T1-T2, μM, median (min, max)	-21.0 (-33.38, …)	9.23 (-5.89, 24.90)	0.071

sNOX2-dp T0-T2, pg/ml, median (min, max)	-3.12 (-17.95, …)	-19.49 (-23.12, -15.79)	0.071

sNOX2-dp = soluble NOX2-derived peptide; ADMA= asymmetric dimethyl-arginine; NO= nitric oxide.

Supplementary Figure 5. Correlations between molecular biomarkers and NIHSS

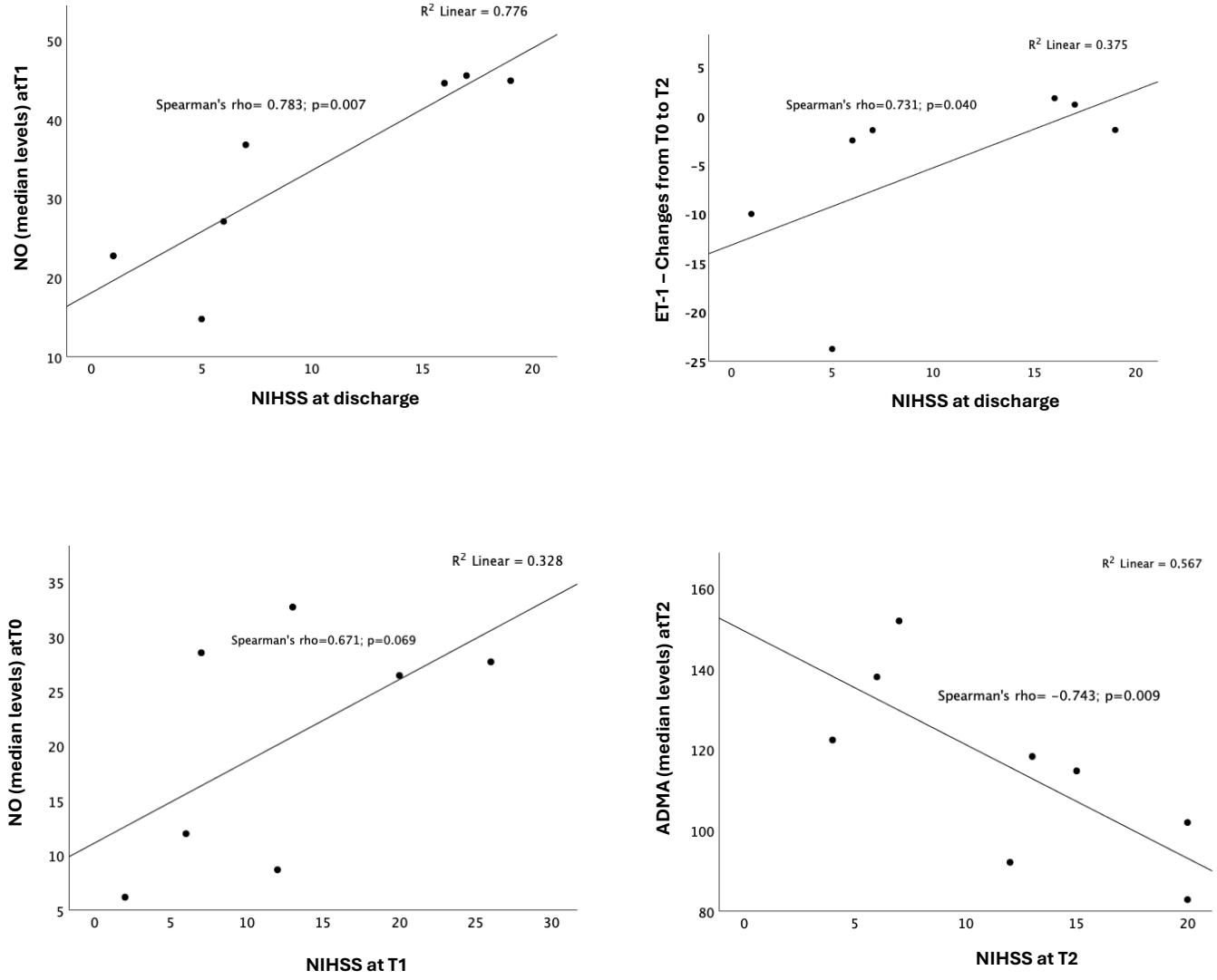

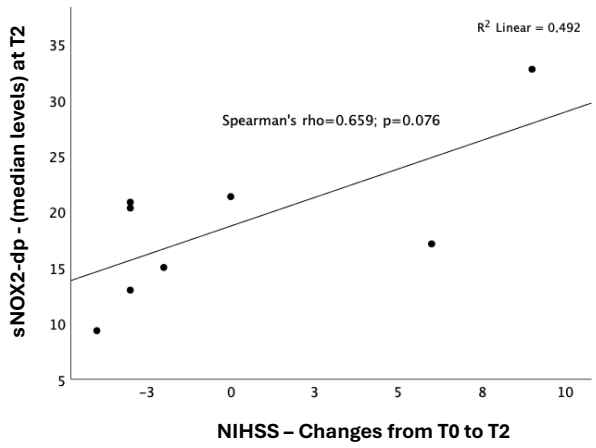

Supplementary Figure 6. Associations between molecular biomarkers and clinical outcome at 3 months

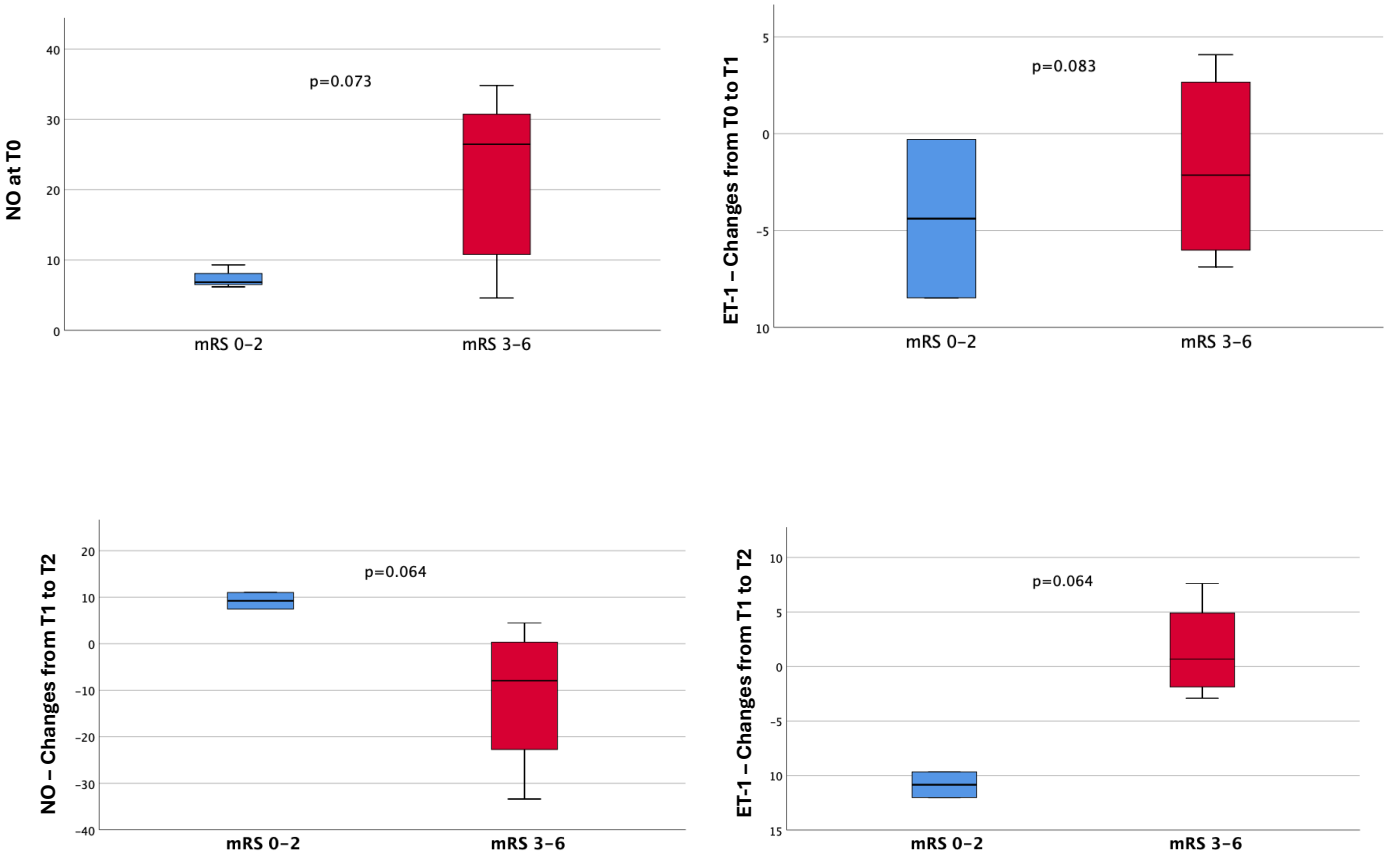

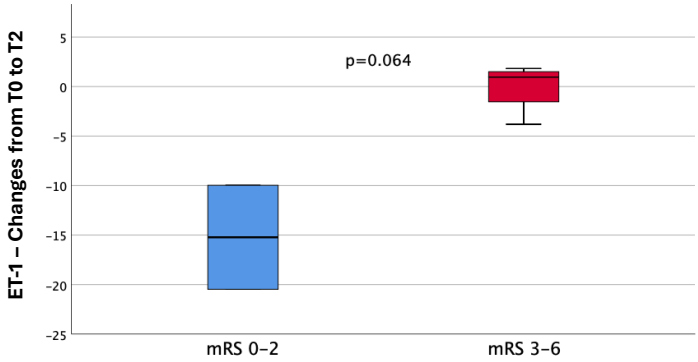

	mRS 0-2 (n=3)	mRS 3-6 (n=3)	p value
NO at T0, median (min, max)	6.85 (6.18, 9.31)	26.46 (34.82, 8.69)	0.073
ET-1 at T0, pg/mL, median (min, max)	29.17 (18.06, 37.20)	17.38 (8.56, 34.83)	0.083
NO T1-T2, µM, median (min, max)	9.23 (7.45, 11.01)	-7.96 (-33.38, 4.45)	0.064
ET-1 T1-T2, pg/mL, median (min, max)	-10.84 (-12.01, -9.67)	0.69 (-2.90, 7.61)	0.064
ET-1 T0-T2, pg/mL, median (min, max)	-15.23 (-20,48, -15.23)	0.96 (-3.81, 1.83)	0.064

mRS=modified Rankin Scale; NO= nitric oxide; ET-1= endothelin 1.

Supplementary Figure 7. Associations between molecular biomarkers intrahospital death

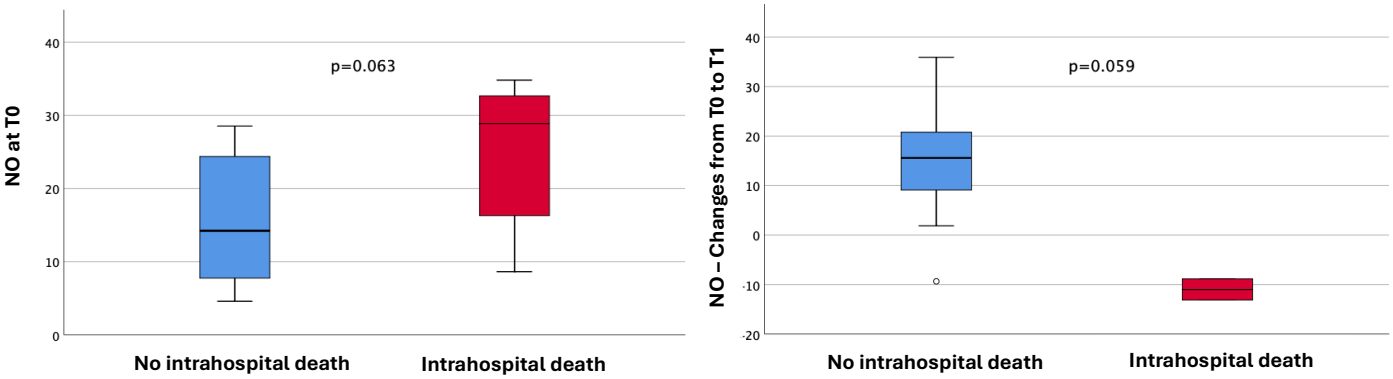

	No intrahospital death (n=11)	Intrahospital death (n=8)	P value
NO at T0, µM, median (min, max)	14.24 (28.54, 28.54)	28.86 (8.65, 34.82)	0.063
NO T0-T1, µM, median (min, max)	15.58 (807.81, 2407.32)	-10.99 (-13.11, -8.86)	0.059

NO= nitric oxide.

Supplementary Figure 8. Associations between molecular biomarkers and death at 3 months

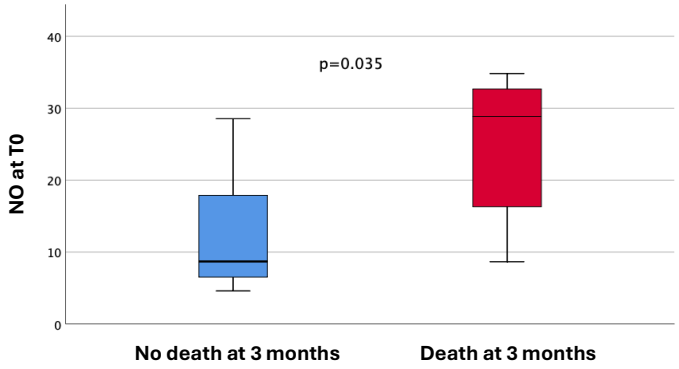

	No death at 3 months (n=7)	Death at 3 months (n=8)	p value
NO at T0, µM, median (min, max)	8.69 (4.61, 28.54)	28.86 (8.65, 34.82)	0.035

NO= nitric oxide.